Article

Not peer-reviewed version

Design, Synthesis, Structural Characterization and Bioactivity of Novel Halolactones Derived from Vanillin: Antiproliferative and Hemolytic Potential

Anna Dunal *, Witold Gładkowski *, Ewa Dejnaka, Joanna Sulecka-Zadka, Aleksandra Pawlak, Aleksandra Włoch, Hanna Pruchnik, Gabriela Maciejewska

Posted Date: 23 July 2025

doi: 10.20944/preprints202507.1965.v1

Keywords: vanillin; lactones; aromatic ring; halolactonization; antiproliferative activity; hemolytic activity

 doi:10.20944/preprints202507.1965.v1

Article

Design, Synthesis, Structural Characterization and Bioactivity of Novel Halolactones Derived from Vanillin: Antiproliferative and Hemolytic Potential

Anna Dunal [1,*], Witold Gładkowski [1,*], Ewa Dejnaka [2], Joanna Sulecka-Zadka [2], Aleksandra Pawlak [2], Aleksandra Włoch [3], Hanna Pruchnik [3] and Gabriela Maciejewska [4]

[1] Department of Food Chemistry and Biocatalysis, Wrocław University of Environmental and Life Sciences, Norwida 25, 50-375 Wrocław, Poland

[2] Department of Pharmacology and Toxicology, Faculty of Veterinary Medicine, Wrocław University of Env ronmental and Life Sciences, Norwida 31, 50-375, Wrocław, Poland

[3] Department of Physics and Biophysics, Faculty of Biotechnology and Food Sciences, Wrocław University of Environmental and Life Sciences, Norwida 25, 50-375, Wrocław, Poland

[4] Omics Research Center, Wrocław Medical University, 50-368 Wrocław, Poland

* Correspondence: anna.dunal@upwr.edu.pl (A.D.); witold.gladkowski@upwr.edu.pl (W.G.)

Abstract

A series of novel γ-halo-δ-lactones and δ-halo-γ-lactones bearing a phenolic ring at the β-position was synthesized from the naturally occurring aromatic aldehyde vanillin. The seven-step synthetic route commenced with benzyl protection of the hydroxy group of the starting material, followed by the synthesis of a γ,δ-unsaturated carboxylic acid, subsequent halolactonization (iodo-, bromo-, and chlorolactonization), and concluded with selective benzyl deprotection. The structures of all synthesized compounds were confirmed by comprehensive spectroscopic analyses, including NMR and HRMS. The resulting halolactones were evaluated for antiproliferative activity against two canine (CLBL-1, CLB70) and two human (T-24, CaCo-2) cancer cell lines, with non-cancerous mouse embryonic fibroblasts (NIH/3T3) serving as controls. Hemolytic assays were performed to assess toxicity toward human red blood cells (RBCs). All compounds demonstrated selective inhibition of cancer cell proliferation, exhibiting no inhibitory effects on normal fibroblasts and no hemolytic toxicity. Among the tested lactones, the *trans* δ-iodo-γ-lactone was the most potent, particularly against CLBL-1 and T-24 cells. These findings underscore the potential of vanillin-derived halolactones as selective anticancer agents with an advantageous safety profile, owing to their lack of toxicity toward non-malignant cells.

Keywords: vanillin; lactones; aromatic ring; halolactonization; antiproliferative activity; hemolytic activity

1. Introduction

Lactones are intramolecular esters of hydroxy acids, found in both natural and synthetic sources. Five- and six-membered lactone rings predominate in nature due to their favorable thermodynamic stability [1]. Natural compounds containing lactone rings are produced mainly by plants [2–4], but also by insects [5], microorganisms [6], and marine organisms [7,8], where they function as secondary metabolites.

This structurally diverse group of compounds exhibits a wide range of biological activities, including antibacterial [9–11], anti-inflammatory [12,13], antifeedant [14–16], and antifungal properties [17–19]. Due to their broad spectrum of bioactivities, lactones are applied in economically important sectors such as the food industry, medicine, and agriculture. Their multifunctional nature makes them attractive candidates for the development of bioactive agents and functional materials.

 doi:10.20944/preprints202507.1965.v1

However, particular attention has been paid to their anticancer properties [20–23]. Numerous studies have been conducted to demonstrate the cytotoxic activity of lactones containing an aromatic substituent against cancer or normal cell lines [24–29]. Selected β-aryl-δ-halo-γ-lactones synthesized from simple aromatic aldehydes exhibit cytotoxicity against human (e.g., Jurkat, HL-60, AGS) and canine (e.g., D17, GL-1, CLBL-1) cancer cell lines [30–33]. The mechanism of action of these compounds involves the induction of apoptosis via a mitochondrial-dependent pathway and caspase activation, as demonstrated for cuminaldehyde-derived δ-iodo-γ-lactones [34]. Enantiomeric *trans* β-aryl-δ-iodo-γ-lactones derived from 2,5-dimethylbenzaldehyde were shown to trigger cancer cell apoptosis by downregulating the anti-apoptotic proteins Bcl-2 and Bcl-xL. In the canine cell lines used in the study, the tested compounds also activated the receptor-mediated apoptotic pathway through fragmentation of the Bid protein, thereby enhancing their pro-apoptotic effects [35]. To gain deeper insight into their biophysical behavior and anticancer mechanisms, enantiomeric piperonal-derived *trans* β-aryl-δ-iodo-γ-lactones have been extensively studied for their ability to induce apoptosis and interact with biological systems, including cancer cell membranes and biomacromolecules. Membrane interaction studies revealed a reduction in membrane fluidity, correlating with a marked induction of apoptosis by these lactones [36]. *Cis* β-aryl-δ-iodo-γ-lactones containing phenyl or *p*-alkyl-substituted phenyl rings exhibited cytotoxic activity against HeLa (human cervix carcinoma) and MCF-7 (human breast adenocarcinoma) cancer cell lines, and significantly disrupted the antioxidative/oxidative balance in the NHDF (normal human dermal fibroblasts) cell line [37].

Continuing our studies on the biological activity of lactones bearing an aromatic ring, we designed and synthesized a series of novel β-arylhalolactones using vanillin **(1)** as the starting material. This naturally occurring aromatic aldehyde has a well-documented spectrum of biological properties, including gastro- and cardioprotective, diuretic, anti-organ toxicity, antimicrobial, anti-inflammatory, neuroprotective, and anti-infective effects, among others [38–40]. Numerous research groups have also reported significant anticancer activity of vanillin **(1)** against various human cancer cell lines, like MCF-7 (breast cancer) [41], HepG2 (hepatocellular carcinoma) [42], HT-29 (colorectal adenocarcinoma) [43], NCI-H460 (non-small cell lung carcinoma) [44], as well as A2058 (malignant melanoma) cell lines [45].

Due to the presence of various reactive functional groups, vanillin **(1)** is also a versatile building block for the synthesis of novel derivatives, including a wide range of heterocyclic systems such as pyrimidines, quinoxalines, imidazoles, and thiazoles, which are highly relevant in medicinal and pharmaceutical chemistry [46]. Vanillin-derived compounds have demonstrated a broad spectrum of pharmacological activities. Notably, hydrazone derivatives of vanillin **(1)** exhibit antimicrobial, anticancer, and enzyme inhibition properties, making them promising candidates for therapeutic applications [47]. Additionally, derivatives bearing tacrine or naphthalimido moieties have been developed as multi-target agents for Alzheimer's disease therapy. These compounds act as antioxidants and inhibit acetylcholinesterase (AChE) as well as β-amyloid peptide aggregation, both of which are key pathological features of Alzheimer's disease [48]. Other vanillin-based derivatives have been designed as dual inhibitors targeting both AChE and butyrylcholinesterase (BuChE), thereby enhancing their potential efficacy in neurodegenerative conditions [49]. Regarding anticancer activity, certain vanillin derivatives-such as compounds based on the SBE13 scaffold significantly outperform the parent compound by potently inducing apoptosis and reducing Plk1 kinase activity in HeLa cells, indicating strong antiproliferative effects [50]. This further emphasizes the potential of vanillin as a versatile scaffold for designing targeted anticancer therapeutics.

The presence of phenolic fragment is an advantageous factor to influence the potential of vanillin-derived halolactones as a promising bioactive compound with different therapeutic properties including cytotoxic, antioxidant, antiinflammatory which can be of high relevance in oncology. Here we would like to present the synthesis and studies on the cytotoxicity of new halolactones obtained from vanillin **(1)** towards different cancer cell lines. Due to the frequently observed high toxicity of anticancer agents towards healthy cells, we also decided to investigate the

 doi:10.20944/preprints202507.1965.v1

hemolytic properties of the synthesized halolactones towards human red blood cells (RBCs). Owing to their simple structure and crucial physiological functions, these cells are a simple and well established model to evaluate general hemolytic potential, as erythrocyte membranes are highly sensitive to chemical induced damage and serve as a convenient indicator of membrane disruptive properties of bioactive compounds.

2. Results and Discussion

2.1. Synthesis of Vanillin-Derived Halolactones

The presence of a reactive phenolic group in the benzene ring of vanillin **(1)** dictated our synthetic strategy, which included the benzyl protection of vanillin **(1)**, the synthesis of the key intermediate γ,δ-unsaturated carboxylic acid **6**, and subsequent halolactonization reactions, followed by a final deprotection step to obtain the target lactones. The use of benzyl protection was essential to prevent side reactions involving the phenolic OH group during the multistep synthesis.

2.1.1. Synthesis of α,β-Unsaturated Carboxylic Acid **6**

The five-step synthesis of γ,δ-unsaturated carboxylic acid **6** is shown on Scheme 1.

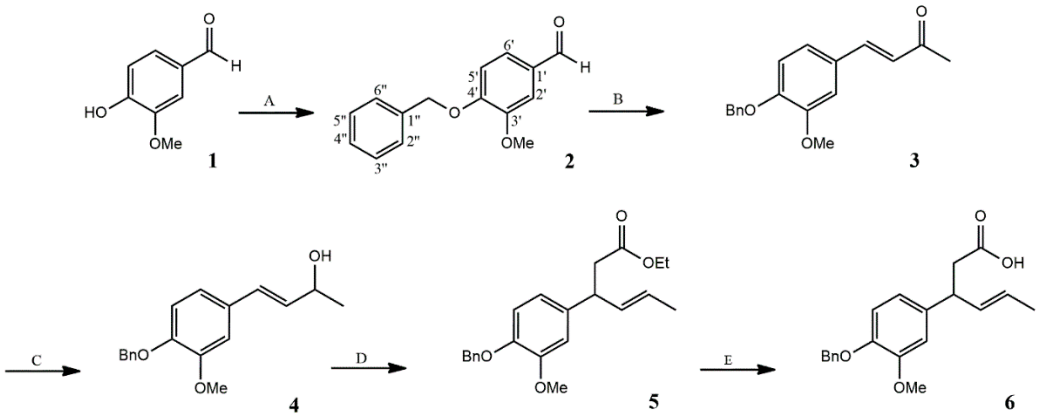

Scheme 1. Synthesis of unsaturated γ,δ-carboxylic acid intermediate **6** from vanillin **(1)**. Reagents and conditions: **(A)** BnBr, K_2CO_3, EtOH, r.t., 48 h **(B)** acetone, 10% NaOH, r.t., 24 h **(C)** MeOH, $NaBH_4$, ice bath 1h, then r.t., 23 h **(D)** triethyl orthoacetate, propionic acid, 138 °C, 6h **(E)** 10% NaOH, EtOH, reflux, 5 h.

Benzylation of vanillin **(1)** was carried out using an ethanolic solution of benzyl bromide in the presence of potassium carbonate. Benzylvanillin **2** was obtained in an 88% yield after crystallization from ethanol. The presence of the benzyl group was confirmed by the ^{1}H NMR spectrum, which showed multiplets in the range of 7.32–7.47 ppm corresponding to the aromatic protons, and a distinctive singlet at 5.21 ppm attributed to the benzylic protons of the methylene group. These characteristic signals provided clear evidence of successful benzyl protection, an essential step for subsequent synthetic transformations.

In the next step, benzylvanillin **2** was converted to the α,β-unsaturated ketone **3** in high yield (84%) via Claisen–Schmidt condensation with acetone under alkaline conditions. The coupling constant between the olefinic protons observed in the ^{1}H NMR spectrum (J = 16.2 Hz) confirmed the *E*-configuration of the C3–C4 double bond.

Reduction of ketone **(3)** by sodium borohydride afforded exclusively the corresponding allylic alcohol **4**. Spectroscopic data confirmed the selective reduction of the carbonyl group, indicated by a multiplet at 4.47 ppm from H-2 and a singlet corresponding to the hydroxyl group at 1.64 ppm, as well as a strong band at 3384 cm^{-1} attributed to O–H stretching vibrations. The retention of the *E*-configured double bond was confirmed by the coupling constant between the H-3 and H-4 protons (J = 15.8 Hz).

 doi:10.20944/preprints202507.1965.v1

Alcohol **4** was subjected to the Johnson–Claisen rearrangement using triethyl orthoacetate in the presence of a catalytic amount of propionic acid at 138 °C. Consistently with the mechanism of Johnson - Claisen rearrangement, *E* configuration of double bond in γ,δ-unsaturated ester **5** was retained, as indicated by the coupling constant (J = 15.3 Hz) between olefinic protons H-4 and H-5. Ester **5**, after two-step purification (first by gravity chromatography and then by flash chromatography) was hydrolyzed in a 10% ethanolic NaOH solution under reflux to afford the γ,δ-unsaturated carboxylic acid **6**.

2.1.2. Halolactonizations of γ,δ-unsaturated Carboxylic Acid **6**

Acid **6** was subjected to halolactonization reactions, leading to the formation of iodo-, bromo-, and chlorolactones as illustrated on Scheme 2.

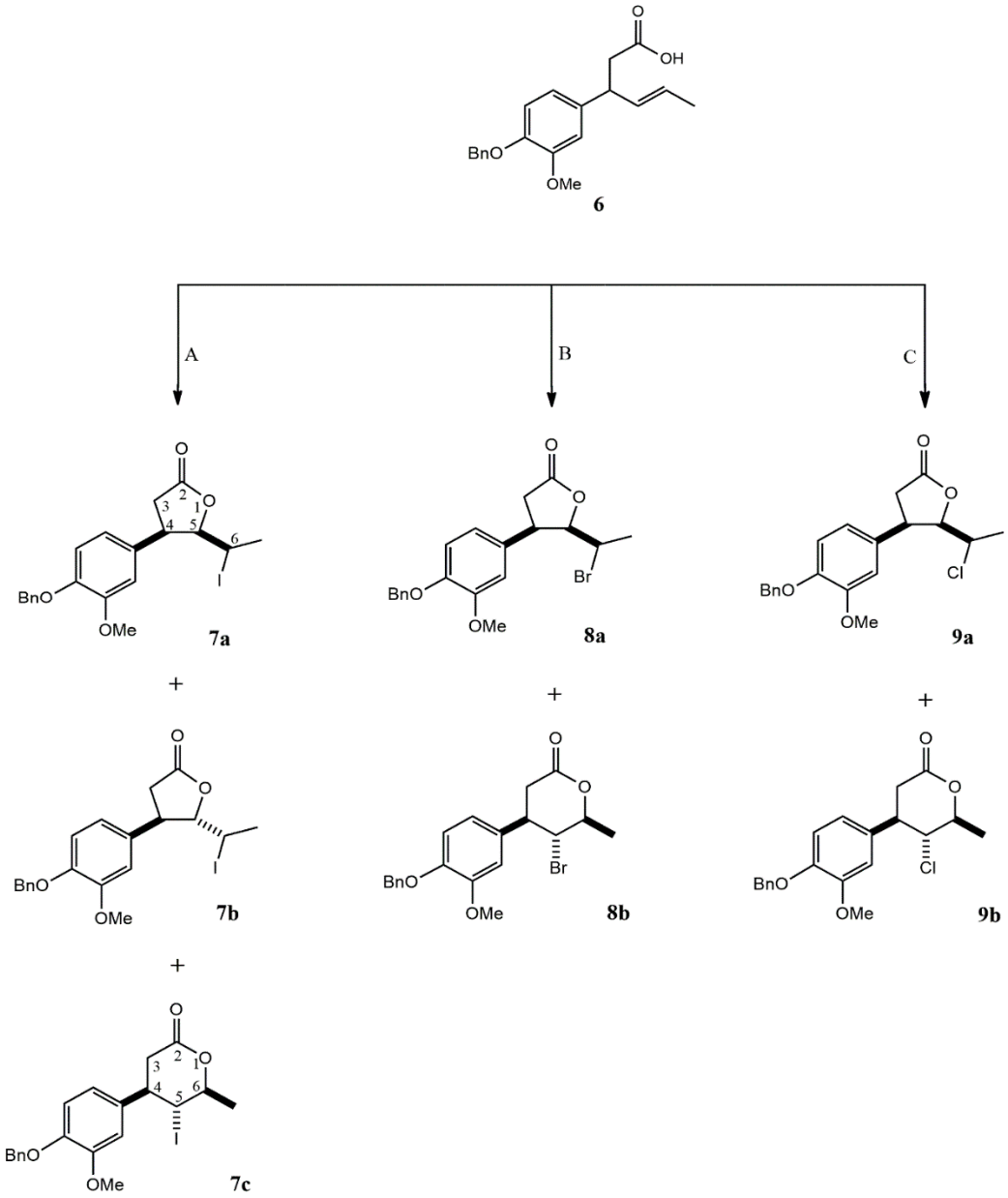

Scheme 2. Halolactonization of acid **6**. Reagents and conditions: **(A)** I_2 in KI, Et_2O, $NaHCO_3$, r.t., 20 h **(B)** NBS, acetic acid, THF, r.t., 24 h **(C)** NCS, acetic acid, THF, r.t., 24 h.

The iodolactonization reaction was carried out using iodine in potassium iodide in a biphasic system $Et_2O/NaHCO_3$. After reaction, three products were successfully isolated and purified by flash

 doi:10.20944/preprints202507.1965.v1

chromatography.

The major isolated products were two γ-lactones obtained as a result of 5-exo cyclization. Spectroscopic analysis (^{1}H NMR) revealed significant differences in the chemical shifts and multiplicities of the H-4, H-5, and H-6 protons, enabling confirmation of the relative orientation of substituents at C-4 and C-5 of the γ-lactone ring. For example, in the case of the cis isomer **7a**, the signal from the H-6 proton was significantly shifted upfield (3.47 ppm) compared to its chemical shift in the trans isomer **7b** (4.36 ppm), which resulted from the location of H-6 within the shielding cone of the aromatic ring. The shape of the multiplet (doublet of quartets) and the coupling constant between H-6 and H-5 (J = 10.9 Hz) indicated an antiperiplanar orientation of the C5–H5 and C6–H6 bonds. For the trans δ-iodo-γ-lactone **7b**, a characteristic triplet at 4.23 ppm from H-5 (J = 5.3 Hz) was observed instead of the doublet of doublets at 4.78 ppm found in the spectrum of the cis isomer.

In the case of the trans δ-iodo-γ-lactone, additional minor signals were observed in the ^{1}H and ^{13}C NMR spectra, resulting from a conformational equilibrium between two conformers: a predominant syn conformer in which the C–I and C–O bonds adopt a "gauche" conformation, and a minor anti conformer where these bonds are arranged in an antiperiplanar orientation. This phenomenon was previously reported and elucidated based on crystallographic analysis by Gładkowski et al. (2013) for analogs of lactone **7b**, namely trans δ-iodo-γ-lactones bearing an unsubstituted phenyl ring at the β-position [31].

In the case of the minor isolated product of 5-endo iodolactonization, γ-iodo-δ-lactone **7c**, the most informative signal was the triplet from the H-5 proton at 4.00 ppm. The coupling constant (J = 10.6 Hz) between the H-4 and H-6 protons observed in the ^{1}H NMR spectrum unequivocally indicated a trans orientation of the iodine at C-5 relative to both the benzene ring at C-4 and the methyl group at C-6.

Bromo- and chlorolactonization of acid **6** were carried out using N-bromosuccinimide (NBS) and N-chlorosuccinimide (NCS), respectively, in anhydrous tetrahydrofuran with a catalytic amount of acetic acid. Both cis δ-bromo-γ-lactone **8a** and cis δ-chloro-γ-lactone **9a**, as well as their corresponding six-membered analogues **8b**, **9b**, were isolated from the product mixtures. However, attempts to isolate the pure stereoisomers of the trans γ-lactones were unsuccessful.

^{1}H NMR data showed a high degree of resemblance in the shapes and coupling constant values of the signals from protons H-4, H-5, and H-6 compared to the corresponding signals observed in the spectra of the analogous iodolactones **7a** and **7c**. Among the halogens, the greatest deshielding effect for protons H-5 and H-6 was observed for iodine, followed by bromine and chlorine, which is consistent with literature data for analogous β-aryl-δ-halo-γ-lactones and β-aryl-γ-halo-δ-lactones [31].

2.1.3. Benzyl Deprotection of Halolactones **7a-c, 8a,b, 9a,b**

The final stage of the synthesis involved the removal of the benzyl protecting group. To identify a selective and efficient method, various deprotection strategies were tested using *cis* δ-iodo-γ-lactone **7a** as a model substrate. The first approach, catalytic hydrogenolysis over Pd/C, was chosen due to its general reliability and operational simplicity in benzyl group removal [51]. However, in this case, the reaction led to a mixture of more polar products than the starting iodolactone **7a**. In search of greater selectivity, **7a** was treated with 33% HBr in acetic acid [52], but the reaction yielded a complex mixture, and GC and NMR analysis indicated isomerization of **7a** to its *trans* isomer **7b**. The resulting products were inseparable by standard purification techniques. Similarly, treatment with concentrated HCl under reflux [53] resulted in a mixture of highly polar products. The use of aqueous $NaBrO_3$ and $Na_2S_2O_3$ solutions [54] also produced a mixture of more and less polar compounds relative to **7a**, that were difficult to separate. Ultimately, the only effective deprotection method involved the use of anhydrous $FeCl_3$ in dry dichloromethane at room temperature under a nitrogen atmosphere [55]. This approach enabled successful removal of the benzyl group, though the initial isolated yield of the final lactone **10a** after flash chromatography was only 10%, likely due to complexation of the phenolic product with Fe^{3+} ions. To improve the yield, during the work-up

 doi:10.20944/preprints202507.1965.v1

procedure reaction mixture was washed with 1% phosphoric(V) acid, following the protocol described by Giri et al. (2020) for $FeCl_3$-mediated deprotection of Boc-protected amino acids and peptides [56]. This modification increased the isolated yield of **10a** to 28%, significantly enhancing the efficiency of the deprotection process.

Following this procedure, successful debenzylation of *cis* δ-halo-γ-lactones **7a**-**9a** and *trans* δ-iodo-γ-lactone **7b** was carried out, affording the corresponding deprotected lactones **10a**-**12a** and **10b**, respectively **(**Scheme 3). The removal of the benzyl group was confirmed by the disappearance of the aromatic proton signals in the range of 7.31–7.47 ppm and the singlet at 5.14–5.15 ppm corresponding to the benzylic methylene protons in the ^{1}H NMR spectra. In place of these, a new singlet appeared at approximately 5.61–5.62 ppm, along with a broad band in the IR spectrum in the range of 3333–3422 cm^{-1}, corresponding to O–H stretching vibrations confirming the presence of a free hydroxy group. Moreover, the successful deprotection was additionally evidenced by the expected molecular masses of the target compounds determined by HRMS analysis. Together, these results provide strong evidence for the complete and selective removal of the benzyl protecting group under the optimized reaction conditions.

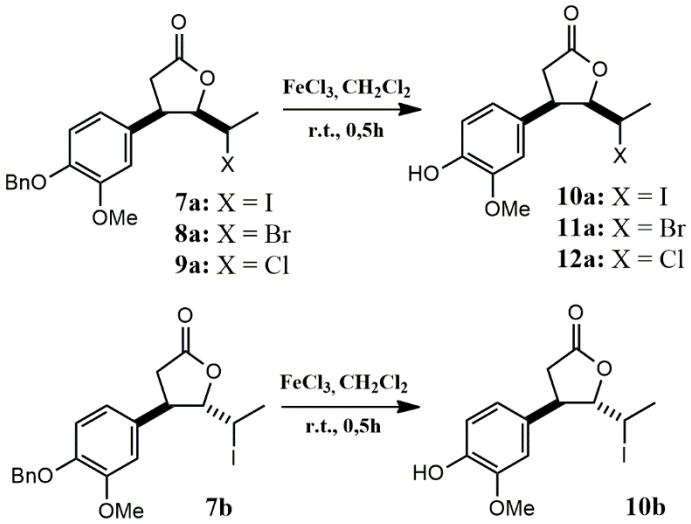

Scheme 3. Debenzylation of cis δ-halo-γ-lactones **7a**-**9a** and trans δ-iodo-γ-lactone **7b**.

An analogous procedure was applied for the deprotection of γ-halo-δ-lactones **7c**, **8b**, and **9b**. Among these, only in the case of γ-chloro-δ-lactone **9b** was a successful deprotection achieved, leading to the isolation of the expected deprotected δ-lactone **12b** as the sole product. Interestingly, NMR analysis of the product obtained from the deprotection of γ-iodo-δ-lactone **7c** clearly confirmed the structure of *trans* δ-iodo-γ-lactone **10b**, suggesting the occurrence of an intramolecular rearrangement through a translactonization process (Scheme 4). In contrast, for the bromo analogue **8b**, TLC and GC analyses revealed the slow formation of two inseparable products, indicating a more complex and less selective reaction course.

 doi:10.20944/preprints202507.1965.v1

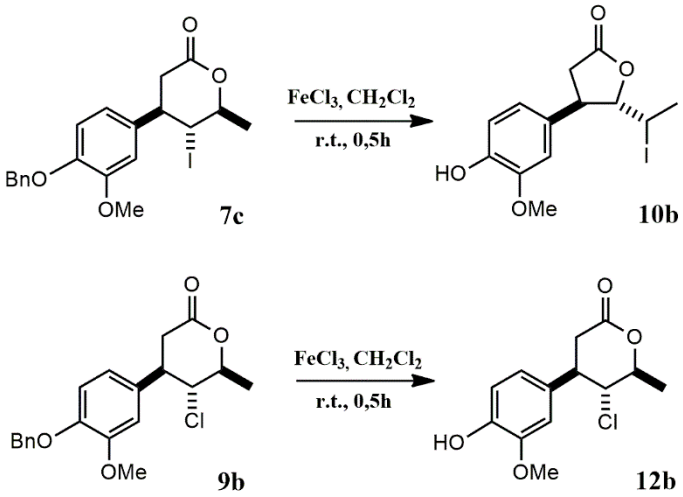

Scheme 4. Debenzylation of γ-halo-δ-lactones **7c** and **9b**.

The proposed mechanism of the translactonization process, which occurs during $FeCl_3$-mediated debenzylation of γ-iodo-δ-lactone **7c**, is illustrated in Scheme 5.

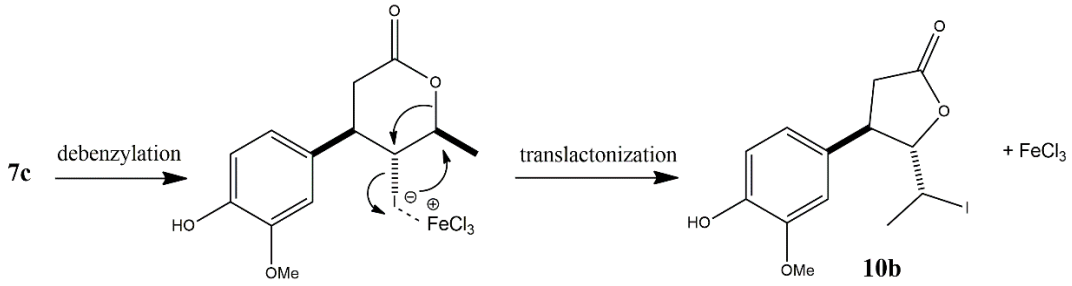

Scheme 5. Proposed translactonization mechanism leading to the formation of trans δ-iodo-γ-lactone **10b** during $FeCl_3$-mediated debenzylation of γ-iodo-δ-lactone **7c**.

The rearrangement appears to proceed in a single step via intramolecular nucleophilic substitution, facilitated by $FeCl_3$. Acting as a Lewis acid, $FeCl_3$ promotes the transposition of the iodine atom from the C-5 to the C-6 position, accompanied by a simultaneous nucleophilic attack of the lactone oxygen on the C-5 carbon, resulting in the formation of a five-membered ring. The exclusive formation of the trans isomer strongly suggests that the substitution follows an S_N2-type mechanism, in which the oxygen nucleophile approaches from the side opposite to the departing iodine atom.

Translactonization converting δ-lactones into γ-lactones has been previously reported in the literature, both under chemical and microbiological halolactonization conditions. Kamizela et al. (2019) observed the unexpected formation of δ-hydroxy-γ-lactones among the products of iodolactonization of 3-methyl-5-arylpent-4-enoic acids using I_2/KI in a biphasic $NaHCO_3/Et_2O$ aqueous system. This phenomenon was attributed to the rearrangement of initially formed γ-iodo-δ-lactones. In that case, the reaction was proposed to proceed via an S_N1-like mechanism, as evidenced by the formation of both cis and trans isomers of the δ-hydroxy-γ-lactones. The process involved a dehalogenation-lactonization sequence with two simultaneous nucleophilic substitutions: replacement of the iodine atom at C-5 by the lactone oxygen, and nucleophilic attack of water at C-6 [24]. Interestingly, in one of our previous studies, a similar rearrangement was observed during the biotransformation of a chalcone-derived γ-bromo-δ-lactone in the culture of Penicillium frequentans AM 359. In contrast to the chemically induced rearrangement, the microbial process proceeded via an S_N2 mechanism, which led exclusively to the formation of a single trans isomer of the hydroxylactone [57].

 doi:10.20944/preprints202507.1965.v1

The translactonization of γ-halo-δ-lactones reported previously typically involved the participation of water, leading to the formation of δ-hydroxy-γ-lactones. In contrast, the $FeCl_3$-mediated debenzylation of γ-iodo-δ-lactone **7c** was carried out under strictly anhydrous conditions, which favored an intramolecular S_N2-type reaction and resulted in the selective formation of the trans δ-iodo-γ-lactone. To the best of our knowledge, this type of rearrangement has not been previously reported and may be attributed to the higher thermodynamic stability of five-membered lactone rings compared to six-membered ones. With regard to the relative reactivity of halogens in the presence of $FeCl_3$, the order can be classified as I > Br > Cl. This trend corresponds to the bond strength between the carbon and halogen atoms, iodine forms the weakest bond, rendering γ-iodo-δ-lactones less stable and more prone to rearrangement. Consequently, no translactonization was observed for γ-chloro-δ-lactone **9b**, and the process occurred only very slowly for its bromo analogue **8b**. Even after 2 h of reaction, TLC analysis revealed the presence of two distinct products, corresponding to the unrearranged δ-lactone and the newly formed γ-lactone.

2.2. Antiproliferative Activity

To evaluate their antiproliferative potential, synthesized vanillin-derived halolactones **10a**,**b**, **11a** and **12a**,**b** as well starting vanillin **(1)** were subjected to *in vitro* MTT assay against panel of selected cancer cell lines: two lines representing hematopoietic canine cancers: canine B-cell lymphoma cell line (CLBL-1) and chronic B-cell leukemia (CLB70) and two human cancer lines: bladder carcinoma (T-24) and colorectal adenocarcinoma (CaCo-2). Normal cell line of mouse embryonic fibroblasts (NIH/3T3) was also used in these studies. The results, expressed as IC_{50} values are shown in Table 1.

Table 1. Antyproliferative activity of vanillin **(1)** and vanillin-derived halolactones **(10a,b**, **11a**, **12a,b)** toward CLBL-1, CLB70, T-24, CaCo-2 and NIH/3T3 cell lines after 72 h of exposure.

Compound	IC_{50} [μg/mL]				
	CLBL-1	**CLB70**	**T-24**	**CaCo-2**	**NIH/3T3**
1	72.44±9.37[1]	72.79±2.28	48.46±13.16	>100	>100
10a	73.55±8.82	69.65±13.69	98.06±10.42	>100	>100
10b	46.26±4.07	71.48±7.47	63.42±6.16	>100	>100
11a	63.18±1.60	76.17±5.30	>100	76.40±9.99	>100
12a	76.67±11.47	75.21±6.25	>100	88.05±4.37	>100
12b	85.72±15.72	71.17±11.64	>100	72.54±19.76	>100

[1] Data represent mean values ± SD from at least four independent experiments.

All tested compounds exhibited measurable antiproliferative activity against the canine cancer cell lines, whereas only three compounds showed notable effects against the human cancer cell lines (T-24 or CaCo-2). This observation suggests a higher susceptibility of hematopoietic canine cancer lines compared to the relatively greater resistance displayed by the human cancer cells towards the tested compounds.

Among the tested compounds, the highest antiproliferative activity was observed for trans γ-iodo-δ-lactone **10b** against the CLBL-1 cell line, with an IC_{50} value of 46.26±4.07 μg/mL, and for vanillin **(1)** against the T-24 cell line (IC_{50} = 48.46±13.16 μg/mL). Moderate activity was also noted for cis γ-bromo-δ-lactone **11a** against CLBL-1 and for compound **10b** against T-24. In all other cases, the tested compounds exhibited lower activity, with IC_{50} values exceeding 70 μg/mL. Importantly, none of the compounds showed cytotoxic effects toward the normal NIH/3T3 fibroblast cell line, indicating

 doi:10.20944/preprints202507.1965.v1

a degree of selectivity toward cancer cells.

Comparing the antiproliferative activity of vanillin **(1)** with its halolactone derivatives against the CLBL-1 cell line, the trans γ-iodo-δ-lactone **10b** and cis γ-bromo-δ-lactone **11a** exhibited notably higher activity. In assays with CaCo-2 cells, vanillin **(1)** was inactive, whereas cis γ-bromo-δ-lactone **11a**, cis γ-chloro-δ-lactone **12a**, and γ-chloro-δ-lactone **12b** demonstrated moderate activity. Conversely, vanillin **(1)** proved to be the most active compound against the T-24 cell line. For the CLB70 line, the antiproliferative activities of vanillin **(1)** and all tested vanillin-derived lactones were comparable.

When evaluating the impact of the halogen substituent on the biological activity of the lactones, iodolactones **10a** and **10b** demonstrated superior activity against the T-24 bladder carcinoma line compared to their bromo- and chlorolactone counterparts (**11a**, **12a** and **12b**). Conversely, for the CaCo-2 colorectal adenocarcinoma line, the trend was reversed, with bromo- and chlorolactones exhibiting relatively higher efficacy than the iodolactones.

Comparing the antiproliferative activity of cis isomers of γ-lactones against hematopoietic cell lines, the highest activity was observed for bromolactone **11a** against the CLBL-1 cell line. In contrast, the activity of all tested cis δ-halo-γ-lactones (**10a**, **11a**, and **12a**) against the CLB70 cell line was comparable. These results clearly indicate that the influence of the halogen substituent on the antiproliferative activity of lactones is strongly dependent on the specific cancer cell line. Similar observations were reported in our previous studies. For instance, when studying a series of racemic halolactones bearing phenyl, p-methylphenyl, and p-isopropylphenyl substituents at the β-position of the lactone ring, bromolactones exhibited higher antiproliferative activity compared to their iodo- and chloro- analogues against the Jurkat cell line (human T-cell leukemia) [31]. In another study, β-aryl-δ-iodo-γ-lactones containing a 2′,5′-dimethylphenyl substituent showed greater activity against the CLBL-1 and D17 (canine osteosarcoma) cell lines, but lower activity against GL-1 (B-cell leukemia) and Jurkat cell lines when compared to their bromo analogs [33].

Considering the effect of the spatial structure of iodolactones on their antiproliferative properties, it is evident that trans δ-iodo-γ-lactone **10b** exhibited considerably higher activity than its cis isomer **10a** against the CLBL-1 and T-24 cell lines, whereas the activities of both isomers against the CLB-70 and CaCo-2 lines were comparable. A higher antiproliferative activity of trans isomers of β-aryl-δ-iodo-γ-lactones, bearing 2,5-dimethylphenyl and 1,3-benzodioxole substituents, compared to their cis isomers was also reported for analogs tested against Jurkat, GL-1, CLBL-1, and D17 cell lines [32].

In summary, among all tested halolactones, the most promising antiproliferative properties were exhibited by trans δ-iodo-γ-lactone **10b**. It showed the highest activity toward the CLBL-1 and T-24 cell lines, and comparable activity against the CLB-70 cell line relative to the other tested halolactones. It is also worth mentioning that structurally related compounds, such as δ-aryl-γ-halo-δ-lactones synthesized from aryl bromides and 3-methylcrotonaldehyde [25], or trans-crotonaldehyde [24], exhibited cytotoxic effects not only toward some cancer cell lines but also against the L929 mouse fibroblast normal cell line. In contrast, in the present study, all tested vanillin-derived halolactones displayed potent and selective antiproliferative activity against cancer cells without affecting the normal NIH/3T3 fibroblast cell line. This favorable selectivity profile makes this group of lactones, particularly lactone **10b**, a promising candidate for further development as a safe anticancer agents.

2.3. Cytotoxicity Toward Red Blood Cells (RBCs)

The next stage of the study focused on determining the toxicity of the tested lactones and vanillin **(1)** toward human red blood cells (RBCs) across a wide concentration range (0 to 200 μM) and at different incubation times (2 h, 24 h, and 72 h).

The results of these analyses are presented as the percentage of hemolysis relative to the control sample without the addition of the tested compound and the sample containing only the solvent -

 doi:10.20944/preprints202507.1965.v1

DMSO, allowing a precise assessment of the compounds' impact. Detailed results are shown in Figure 1 and Table 2.

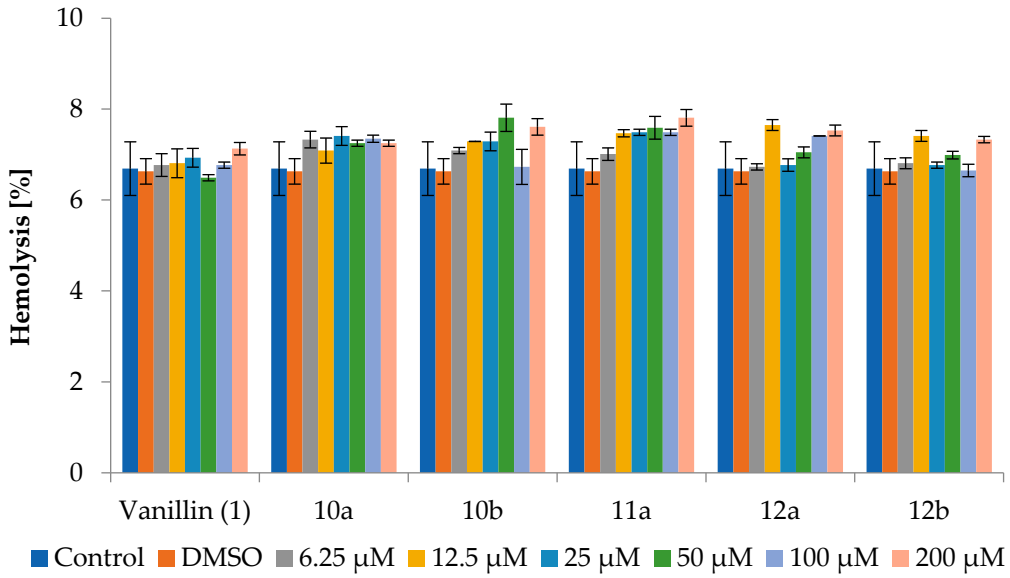

Figure 1. Percentage of hemolysis after 2 h in the presence of the compounds. Error bars represent mean ±SD (n=3).

Table 2. Percentage of hemolysis after 24 h and 72 h in the presence of of vanillin **(1)** and vanillin-derived halolactones **(10a,b**, **11a**, **12a,b)**.

				24 h				
[µM]	**Vanillin (1)**	**10a**	**10b**	**11a**	**12a**	**12b**	**DMSO**	**Control**
6.25	8.05±0.15[1]	7.70±0.07	7.61±0.13	8.50±0.15	8.10±0.0	7.34±0.06	7.92±0.07	7.65±0.44
12.50	7.47±0.15	7.83±0.51	7.87±0.07	8.10±0,15	7.52±0.32	7.47±0.06		
25	7.25±0.13	7.95±0.13	7.74±0.48	7.78±0.33	7.43±0.48	7.83±0.06		
50	7.16±0.60	7.30±0.19	8.45±0.07	7.83±0.07	7.78±0.13	7.96±0.80		
100	7.87±0.26	7.70±0.51	7.92±0.15	8.05±0.07	8.41±0.07	7.87±0.06		
200	8.01±0.13	8.41±0.07	8.50±0.19	8.99±0.69	7.70±0.26	8.01±0.06		
				72 h				
6.25	9.10±0.15	9.22±0.15	9.65±0.15	9.09±0.09	9.06±0.46	8.77±0.15	9.58±0.79	9.26±0.93
12.50	9.21±0.31	9.38±0.09	8.94±0.57	9.25±0.38	8.98±0.00	9.04±0.69		
25	9.21±0.15	9.43±0.30	9.17±0.15	8.99±0.01	9.74±0.53	9.59±0.52		
50	9.54±0.40	8.86±0.17	9.75±0.40	9.87±0.01	9.03±0.09	9.08±0.09		
100	9.42±0.23	9.26±0.38	9.66±0.65	9.16±0.09	8.71±0.17	9.15±0.09		

 doi:10.20944/preprints202507.1965.v1

200	10.22±0.15	9.92±0.35	11.00±0.90	10.34±1.20	9.67±0.80	10.52±0.75

[1] Data represent mean values ± SD from at least three independent experiments.

The results showed that incubation of red blood cells with vanillin **(1)** and the tested lactones **10a**,**b**, **11a**, **12a**,**b** for 2 h showed hemolysis between 6.65±0.14% and 7.81±0.18%, regardless of the concentration, with hemolysis levels for DMSO and control sample 6.69±0.59% and 6.63±0.28%, respectively.

A slight increase in the percentage of hemolysis was observed after 24 h of incubation, with values ranging from 7.30±0.19% to 8.99±0.69%, especially for **10a** and **11a** at the highest concentrations. However, that the level of hemolysis for the control and with DMSO was similar to each other, with values of 7.65±0.44% and 7.92±0.07%, respectively.

After 72 h of incubation, hemolysis increased slightly in all samples to above 9%. It was also observed that for three lactones - **10b**, **11a** and **12b** at the highest concentration, the level of hemolysis was slightly higher compared to the other compounds and the control and amounted to 11.00±0.90%, 10.34±1.20% and 10.52±0.75%, respectively. The results obtained indicate a slight hemolytic effect associated with the prolonged incubation and very high concentration (200 μM) of the tested compounds. Nevertheless, the percentage of hemolysis increased by less than 2% compared to the control and DMSO.

The results of the study demonstrate that over a wide range of concentrations (exceeding those used in cell line studies), both vanillin and all tested vanillin-derived halolactones did not exhibit a significant increase in hemolysis compared to the control and DMSO after 2 and 24 h of exposure. Although prolonged exposure to high concentrations caused minor hemolytic effects for some halolactones, the values remained only slightly elevated relative to the control and DMSO, suggesting that the tested compounds should be considered non-toxic to erythrocytes. It should also be emphasized that hemolysis values for both DMSO and the control remained at the same level, confirming that the solvent itself had no impact on erythrocyte integrity.

The hemolytic activity profile of the tested lactones observed in this study is strongly supported by previous investigations of structurally related compounds, which likewise demonstrated no-toxic effects on erythrocyte membranes. Włoch et al. (2020) examined racemic β-aryl-δ-iodo-γ-lactones with various aromatic substituents and showed that bromolactone analogues, bearing either a methyl group or no substituent on the benzene ring, did not induce hemolysis in erythrocytes even after 48 h of incubation [37].

In another study, Włoch et al. (2025) also evaluated the toxicity of enantiomeric piperonal-derived trans β-aryl-δ-iodo-γ-lactones toward human red blood cells (RBCs) across a wide range of concentrations and various incubation times [36]. In this case as well, the results demonstrated a lack of toxicity at the tested concentrations and extended incubation periods. However, it should be noted that in both cited studies the concentration range examined (up to 100 μM) was significantly lower than in the present work. Furthermore, the incubation time in our study was longer (up to 72 h) compared to those previous reports (up to 48 h).

3. Materials and Methods

2.3. Chemicals

Vanillin (99% purity), benzyl bromide (98% purity), anhydrous methylene chloride (≥99.8% purity), anhydrous iron(III) chloride (98% purity), *N*-bromosuccinimide (NBS) (95% purity), *N*-chlorosuccinimide (NCS) (98% purity), sodium borohydride (≥96% purity), anhydrous tetrahydrofuran (THF) (≥99% purity), triethyl orthoacetate (97% purity), were purchased from Merck (Darmstadt, Germany). Other common reagents and solvents were purchased from Chempur (Piekary Śląskie, Poland or Idalia Radom, Poland).

3.2. Analysis and Purification

 doi:10.20944/preprints202507.1965.v1

The reaction progress was monitored by Thin Layer Chromatography (TLC) using 0.2 mm aluminum plates coated with silica gel 60 F254 (Merck, Darmstadt, Germany). Chromatograms were visualized by spraying the plates with a 1% solution of $Ce(SO_4)_2$ and 2% $H_3[P(Mo_3O_{10})_4]$ in 10% H_2SO_4, followed by heating the plates at 120-200 °C.

Gas Chromatography (GC) analysis was conducted using an Agilent Technologies 6890N (Santa Clara, CA, USA) instrument equipped with an autosampler, split injection (50:1), and an FID detector, employing a DB5-HT column (Agilent, Santa Clara, CA, USA), polyimide-coated fused silica tubing, 30 m x 0.25 mm x 0.10 μm with hydrogen as the carrier gas. For analysis of lactones **10a,b**, **11a, 12a,b**, the following temperature program was used: injector and detector (FID) temperatures 300 °C, the column temperature was programmed from 100 °C to 200 °C at a rate of 20 °C/min, followed by a ramp from 200 °C to 300 °C at 30 °C/min, with a hold at 300 °C for 8 minutes. For intermediate product analysis **1-5**, the initial column temperature was 100 °C, followed by a temperature increase from 100 °C to 200 °C at a rate of 20 °C/min, then from 200 °C to 300 °C at a rate of 30 °C/min, and finally a 1-minute hold at 300 °C.

Nuclear Magnetic Resonance (NMR) spectra, including ^{1}H NMR, ^{13}C NMR, ^{13}C DEPT 135, COSY, HMQC and HMBC were recorded using either a Jeol 400 MHz Year Hold Magnet spectrometer (Jeol Ltd., Tokyo, Japan) or NMR Avance III HD 600 MHz spectrometer (Bruker Biospin GmbH, Rheinstetten, Germany). They are available in the *Supplementary Materials* **(Fig. S1–S102)**. Samples were dissolved in $CDCl_3$ (≥ 99%) or CD_3OD (≥ 99%) and chemical shifts were referenced to the residual solvent signal (δ_H = 7.26, δ_C = 77.00 or δ_H = 3.31, δ_C = 49.00).

Infrared (IR) spectra were acquired using a Nicolet iS10 FTIR Spectrometer (Thermo Fisher Scientific™, Waltham, MA, USA), equipped with a monolithic diamond ATR crystal attachment. All recorded IR spectra are available in the *Supplementary Materials* **(Fig. S103-S119)**.

High Resolution Mass Spectra (HRMS) were recorded on either a Bruker Daltonics ESI-Q-TOF maXis impact mass spectrometer (Bruker, Billerica, MA, USA) or a Waters Xevo G2 mass spectrometer (Waters, Milford, MA, USA), with positive or negative electrospray ionization (ESI) techniques.

Flash chromatography was conducted using the puriFlash® SX520 Plus system (Interchim, Montluçon, France), which includes a gradient pump, UV detector, and fraction collector. Samples were dry loaded on a pre-column (puriFlash®) and the compounds were separated on puriFlash® SIHP F0012 or F0040 30 μm columns by gradient elution with hexane/ethyl acetate mixtures (flow rate: 26 mL/min; pressure: 15 mbar).

The melting points (uncorrected) were determined on the Boetius apparatus (Nagema, Dresden, Germany).

3.3. Preparation of Benzylvanillin **(2)**

Vanillin **(1)** (5.00 g, 33.86 mmol), potassium carbonate (5.26 g, 38.06 mmol), and benzyl bromide (4.90 mL, 41.27 mmol) were dissolved in ethanol (150 mL) and stirred at room temperature for 48 h. The reaction mixture was then filtered to remove solid impurities, and the solvent was evaporated under reduced pressure. The resulting residue was treated with 30 mL of 5% aqueous NaOH and the product was extracted with methylene chloride (3 × 30 mL). The combined organic layers were dried over anhydrous $MgSO_4$, filtered, and the solvent was removed under reduced pressure. The crude product was dissolved in hot ethanol and recrystallized by cooling at –20 °C for 72 h. The resulting crystals were collected by vacuum filtration using a Büchner funnel, washed with cold ethanol, and dried to afford pure benzylvanillin **(2)**, which was characterized by the following physical and spectral data:

Yield 7.01 g (88%); light yellow crystals; mp 58-60 °C (lit. 61-63 °C) [58]; R_f = 0.45 (hexane/ethyl acetate 3:1, *v*/*v*); ^{1}H NMR (400 MHz, CD_3OD): δ 3.90 (s, 3H, -OCH_3), 5.21 (s, 2H, -OCH_2Ph), 7.17 (d, *J* = 8.2 Hz, 1H, H-5'), 7.32 (m, 1H, H-4''), 7.35 – 7.40 (m, 2H, H-3'', H-5''), 7.43 – 7.47 (m, 3H, H-2', H-2'' and H-6''), 7.49 (dd, *J* = 8.2 and 1.9 Hz, 1H, H-6'), 9.80 (s, 1H, -CHO); ^{13}C NMR (100 MHz, CD_3OD): δ 56.44 (-OCH_3), 71.82 (-OCH_2Ph), 111.00 (C-2), 113.91 (C-5), 127.49 (C-6), 128.69 (C-2',C-6'), 129.17 (C-

 doi:10.20944/preprints202507.1965.v1

4′), 129.59 (C-3′,C-5′), 131.71 (C-1), 137.84 (C-1′), 151.50 (C-3), 155.33 (C-4), 192.94 (-CHO); IR (ATR): ν_{max} = 2840, 1676, 1584, 1506, 1262, 1134, 748 cm^{-1}; HRMS (ESI): *m*/*z* calcd for $C_{15}H_{14}O_3$ $[M+Na]^+$: 265.0835; found: 265.0837.

*3.4. Preparation of Ketone **3** via Claisen–Schmidt Condensation*

A solution of benzylvanillin **(2)** (7.01 g, 28.96 mmol) in acetone (230 mL) was stirred in a water bath. A 10% aqueous NaOH solution (20 mL) was added dropwise to the reaction mixture. The reaction was stirred at room temperature for 24 h, after which the mixture was acidified to pH = 2 using 1 M HCl. The resulting product was extracted with methylene chloride (3 × 40 mL). The combined organic layers were washed with brine, dried over anhydrous $MgSO_4$, and filtered. The solvent was removed under reduced pressure, and the crude product was purified by flash chromatography (gradient elution from hexane to hexane/ethyl acetate 7:1, *v*/*v*) to afford pure (*E*)-4-(4'-(benzyloxy-3'-methoxyphenyl)but-3-en-2-one **(3)**, which was characterized by the following physical and spectral data:

Yield 6.86 g (84%); yellow crystals; mp 91-93 °C (lit. 92-93 °C) [59]; R_f = 0.21 (hexane/ethyl acetate 4:1, *v*/*v*); ^{1}H NMR (400 MHz, $CDCl_3$): δ 2.36 (s, 3H, CH_3-1), 3.92 (s, 3H, -OCH_3), 5.19 (s, 2H, -OCH_2Ph), 6.59 (d, *J* = 16.2 Hz, 1H, H-3), 6.88 (d, *J* = 8.3 Hz, 1H, H-5′), 7.05 (dd, *J* = 8.3 Hz and 2.0 Hz, 1H, H-6′), 7.09 (d, *J* = 2.0 Hz, 1H, H-2′), 7.31 (m, 1H, H-4′′), 7.35-7.40 (m, 2H, H-3′′, H-5′′), 7.41-7.45 (m, 2H, H-2′′, H-6′′), 7.44 (d, *J* = 16.2 Hz, H-4); ^{13}C NMR (100 MHz, $CDCl_3$): δ 27.31 (C-1), 55.95 (-OCH_3), 70.78 (-OCH_2Ph), 110.12 (C-2′), 113.34 (C-5′), 122.74 (C-6′), 125.31 (C-3), 127.16 (C-2′′,C-6′′), 127.61 (C-1′), 128.01 (C-4′′), 128.61 (C-3′′, C-5′′), 136.44 (C-1′′), 143.46 (C-4), 149.76 (C-3′), 150.43 (C-4′), 198.35 (C-2); IR (ATR): ν_{max} = 1661, 1637, 1514, 1255, 1142, 974, 839, 806, 744, 697 cm^{-1}; HRMS (ESI): *m*/*z* calcd for $C_{18}H_{18}O_3$ $[M+Na]^+$: 305.1148; found: 305.1155.

*3.5. Preparation of Allylic Alcohol **4***

Ketone **3** (6.86 g, 24.32 mmol) was dissolved in methanol (200 mL), and the solution was cooled in an ice bath. An aqueous solution of $NaBH_4$ (2.05 g in 12 mL H_2O) was added dropwise to the stirred reaction mixture. The reaction was stirred for 1 h in the ice bath and then for 23 h at room temperature. After this time, hot water (150 mL) was added, and the product was extracted with methylene chloride (3 × 30 mL). The organic layer was washed with brine, dried over anhydrous $MgSO_4$, and filtered. The solvent was removed under reduced pressure to afford pure (*E*)-4-(4'-benzyloxy-3'-methoxyphenyl)but-3-en-2-ol **(4)**, which was characterized by the following physical and spectral data:

Yield 5.67 g (82%); white solid; mp 55-57 °C; R_f = 0.25 (hexane/acetone 3:1, *v*/*v*); ^{1}H NMR (400 MHz, $CDCl_3$): δ 1.37 (d, *J* = 6.4 Hz, 3H, CH_3-1), 1.64 (s, 1H, -OH), 3.91 (s, 3H, -OCH_3), 4.47 (m, 1H, H-2), 5.16 (s, 2H, -OCH_2Ph), 6.13 (dd, *J* = 15.8 Hz and 6.6 Hz, 1H, H-3), 6.48 (d, *J* = 15.8 Hz, 1H, H-4), 6.82 (d, *J* = 8.2 Hz, 1H, H-5′), 6.85 (dd, *J* = 8.2 and 1.6 Hz, 1H, H-6′), 6.96 (d, *J* = 1.6 Hz, 1H, H-2′), 7.30 (m, 1H, H-4′′), 7.33-7.39 (m, 2H, H-3′′, H-5′′), 7.40-7.46 (m, 2H, H-2′′, H-6′′); ^{13}C NMR (100 MHz, $CDCl_3$): δ 23.44 (C-1), 55.91 (OCH_3), 69.02 (C-2), 70.92 (-OCH_2Ph), 109.25 (C-2′), 113.80 (C-5′), 119.52 (C-6′), 127.19 (C-2′′, C-6′′), 127.81 (C-4′′), 128.52 (C-3′′, C-5′′), 129.19 (C-4), 130.15 (C-1′), 131.75 (C-3), 136.99 (C-1′′), 147.91 (C-4′), 149.62 (C-3′); IR (ATR): ν_{max} = 3384, 1513, 1264, 1139, 969, 798, 858, 744, 699 cm^{-1}; HRMS (ESI): *m*/*z* calcd for $C_{18}H_{20}O_3$ $[M+Na]^+$: 307.1305; found: 307.1317.

*3.6. Preparation of Ester **5** by Johnson-Claisen Rearrangement*

A mixture of alcohol **4** (5.67 g, 19.94 mmol), triethyl orthoacetate (230 mL, 1.27 mol), and a few drops of propionic acid was heated at 138 °C for 6 h with continuous distillation of ethanol. Upon completion of the reaction (monitored by TLC), the mixture was subjected to silica gel column chromatography to remove excess triethyl orthoacetate (eluent: hexane/acetone 10:1, *v*/*v*). The crude product was further purified by flash chromatography (gradient elution from hexane to hexane/ethyl

 doi:10.20944/preprints202507.1965.v1

acetate 19:1, *v*/*v*) to afford pure (*E*)-3-(4'-benzyloxy-3'-methoxyphenyl)hex-4-enoate **(5)**, which was characterized by the following physical and spectral data:

Yield 3.32 (47%); light yellow oily liquid; R_f = 0.64 (hexane/ethyl acetate (3:1, *v*/*v*); ^{1}H NMR (400 MHz, $CDCl_3$): δ 1.17 (t, *J* = 7.1 Hz, 3H, -$OCH_2\underline{C}H_3$), 1.65 (d, *J* = 6.0 Hz, 3H, CH_3-6), 2.62 (dd, *J* = 14.8 and 7.5 Hz, 1H, one of CH_2-2), 2.66 (dd, *J* = 14.8 and 8.0 Hz, 1H, one of CH_2-2), 3.73 (m, 1H, H-3), 3.88 (s, 3H, -OCH_3), 4.04-4.10 (two q, *J* = 7.1 Hz, 2H, -$OC\underline{H}_2CH_3$), 5.12 (s, 2H, -OCH_2Ph), 5.48 (dq, *J* = 15.3 and 6.0 Hz, 1H, H-5), 5.57 (ddq, *J* = 15.3, 7.1 and 1.1 Hz, 1H, H-4), 6.68 (dd, *J* = 8.2 and 2.0 Hz 1H, H-6′), 6.75 (d, *J* = 2.0 Hz, 1H, H-2′), 6.81 (d, *J* = 8.2 Hz, H-5′), 7.29 (m, 1H, H-4′′), 7.32-7.39 (m, 2H, H-3′′, H-5′′), 7.40-7.45 (m, 2H, H-2′′, H-6′′); ^{13}C NMR (100 MHz, $CDCl_3$): δ 14.19 (-$OCH_2\underline{C}H_3$), 17.89 (C-6), 41.18 (C-2), 44.57 (C-3), 55.98 (-OCH_3), 60.26 (-OCH_2CH_3), 71.07 (-$O\underline{C}H_2$Ph), 111.38 (C-2′), 114.06 (C-5′), 119.12 (C-6′), 125.42 (C-5), 127.22 (C-2′′, C-6′′), 127.73 (C-4′′), 128.47 (C-3′′, C-5′′), 133.17 (C-4), 136.61 (C-1′), 137.32 (C-1′′), 146.75 (C-4′), 149.53 (C-3′), 172.03 (C-1); IR (ATR): ν_{max} = 1731, 1511, 1259, 1137, 1025, 967, 852, 802, 734, 696 cm^{-1}; HRMS (ESI): *m*/*z* calcd for $C_{22}H_{26}O_4$ [M+Na]$^+$: 377.1723; found: 377.1740.

3.7. Preparation of Acid ***6***

Ester **5** (3.32 g, 9.37 mmol) was heated under reflux for 5 h in a 10% ethanol solution of NaOH (230 mL). After evaporating the solvent under reduced pressure, the residue was diluted with water, and organic impurities were removed by extraction with diethyl ether (3 × 30 mL). The aqueous layer was acidified with 1M HCl, and the product was extracted with methylene chloride (3 × 30 ml). The combined organic layers were washed with brine, dried over anhydrous $MgSO_4$, and the solvent was evaporated in *vacuo* to afford pure (*E*)-3-(4'-benzyloxy-3'-methoxyphenyl)hex-4-enoic acid **(6)** with the following physical and spectral data:

Yield 2.51 g (82%); white solid; mp 95-98 °C; R_f = 0.05 (hexane/ethyl acetate 3:1, *v*/*v*); ^{1}H NMR (400 MHz, $CDCl_3$): δ 1.66 (d, *J* = 5.8 Hz, 3H, CH_3-6), 2.68 (dd, *J* = 15.6 and 7.4 Hz, 1H, one of CH_2-2), 2.72 (dd, *J* = 15.6 and 8.0 Hz, 1H, one of CH_2-2), 3.72 (m, 1H, H-3), 3.87 (s, 3H, -OCH_3), 5.12 (s, 2H, -OCH_2Ph), 5.50 (dq, *J* = 15.4 and 5.8 Hz, 1H, H-5), 5.57 (ddq, *J* = 15.4, 6.8 and 1.2 Hz, 1H, H-4), 6.68 (dd, *J* = 8.2 and 2.0 Hz 1H, H-6′), 6.74 (d, *J* = 2.0 Hz, 1H, H-2′), 6.82 (d, *J* = 8.2 Hz, H-5′), 7.29 (m, 1H, H-4′′), 7.33-7.39 (m, 2H, H-3′′, H-5′′), 7.40-7.45 (m, 2H, H-2′′, H-6′′); ^{13}C NMR (100 MHz, $CDCl_3$): δ 17.91 (C-6), 40.67 (C-2), 44.06 (C-3), 55.98 (-OCH_3), 71.05 (-OCH_2Ph), 111.36 (C-2′), 114.02 (C-5′), 119.06 (C-6′), 125.68 (C-5), 127.23 (C-2′′, C-6′′), 127.76 (C-4′′), 128.49 (C-3′′, C-5′′), 132.88 (C-4), 136.25 (C-1′), 137.26 (C-1′′), 146.86 (C-4′), 149.54 (C-3′), 177.57 (C-1); IR (ATR): ν_{max} = 2500-3500, 1702, 1518, 1236, 1142, 965, 855, 791, 744, 696 cm^{-1}; HRMS (ESI): *m*/*z* calcd for $C_{20}H_{22}O_4$ [M+Na]$^+$: 349.1410; found: 349.1413.

3.8. Preparation of Iodolactones ***7a-c***

A solution of acid **6** (2.69 g, 7.70 mmol) in diethyl ether (80 mL) and saturated $NaHCO_3$ solution (80 mL) was stirred for 1 h at room temperature. Then, a solution of I_2 (12.70 g, 50.01 mmol) and KI (3.97 g, 23.92 mmol) in water (20 mL) was added dropwise to the stirred mixture until a stable brown color was observed. After 19 h, the reaction mixture was diluted with diethyl ether and washed with aqueous $Na_2S_2O_3$. The aqueous phase was shaked with diethyl ether (3 × 30 mL), and the combined organic layers were washed with saturated $NaHCO_3$, brine, then dried over anhydrous $MgSO_4$. After evaporation of the solvent under reduced pressure, the mixture of iodolactones was separated by flash chromatography (gradient elution from hexane to hexane/ethyl acetate 5:1, *v*/*v*). Physicochemical and spectral data of the isolated iodolactones **7a–c** are given below:

3.8.1. *Cis*-4-(4'-benzyloxy-3'-methoxyphenyl)-5-(1-iodoethyl)dihydrofuran-2-one **(7a)**

Yield 1.81 g (52%); white solid; mp 116-118 °C; R_f = 0.27 (hexane/ethyl acetate 4:1, *v*/*v*); ^{1}H NMR (400 MHz, $CDCl_3$): δ 2.01 (d, *J* = 6.8 Hz, 3H, CH_3-7), 2.70 (d, *J* = 17.5 Hz, 1H, one of CH_2-3), 3.10 (dd, *J* = 17.5 and 8.4 Hz, 1H, one of CH_2-3), 3.47 (dq, *J* = 10.9 and 6.8 Hz, 1H, H-6), 3.84 (dd, *J* = 8.4 and 5.0

 doi:10.20944/preprints202507.1965.v1

Hz, 1H, H-4), 3.89 (s, 3H, -OCH_3), 4.78 (dd, *J* = 10.9 and 5.0 Hz, 1H, H-5), 5.14 (s, 2H, -OCH_2Ph), 6.71 (dd, *J* = 8.3 and 2.1 Hz, 1H, H-6′), 6.80-6.86 (m, 2H, H-2′, H-5′), 7.31 (m, 1H, H-4′′), 7.34-7.40 (m, 2H, H-3′′, H-5′′), 7.41-7.46 (m, 2H, H-2′′, H-6′′); ^{13}C NMR (100 MHz, $CDCl_3$): δ 23.70 (C-6), 25.53 (C-7), 38.83 (C-3), 44.54 (C-4), 56.04 (-OCH_3), 70.98 (-OCH_2Ph), 87.87 (C-5), 112.80 (C-2′), 113.87 (C-5′), 120.26 (C-6′), 127.31 (C-2′′, C-6′′), 127.93 (C-4′′), 128.57 (C-3′′, C-5′′), 130.05 (C-1′), 136.86 (C-1′′), 147.81 (C-4′), 149.31 (C-3′), 176.64 (C-2); IR (ATR): ν_{max} = 1789, 1518, 1239, 1148, 1012, 954, 857, 751, 700, 538 cm^{-1}; HRMS (ESI): *m*/*z* calcd for $C_{20}H_{21}IO_4$ $[M+Na]^+$ 475.0377; found: 475.0390.

3.8.2. *Trans*-4-(4'-benzyloxy-3'-methoxyphenyl)-5-(1-iodoethyl)dihydrofuran-2-one **(7b)**

Yield 0.87 g (25%); white solid; mp 80-82 °C; R_f = 0.16 (hexane/ethyl acetate 4:1, *v*/*v*); ^1H NMR (400 MHz, $CDCl_3$): major signals from *syn* conformer: δ 1.86 (d, *J* = 7.1 Hz, 3H, CH_3-7), 2.64 (dd, *J* = 18.4 and 6.6 Hz, one of CH_2-3), 3.12 (dd, *J* = 18.4 and 10.0 Hz, 1H, one of CH_2-3), 3.56 (ddd, *J* = 10.0, 6.6 and 5.3 Hz, 1H, H-4), 3.89 (s, 3H, -OCH_3), 4.23 (t, *J* = 5.3 Hz, 1H, H-5), 4.36 (qd, *J* = 7.1 and 5.3 Hz, 1H, H-6), 5.14 (s, 2H, -OCH_2Ph), 6.73 (dd, *J* = 8.2 and 2.1 Hz, 1H, H-6′), 6.75 (d, *J* = 2.1 Hz, 1H, H-2′), 6.85 (d, *J* = 8.2 Hz, 1H, H-5′), 7.31 (m, 1H, H-4′′), 7.34-7.40 (m, 2H, H-3′′, H-5′′), 7.41-7.45 (m, 2H, H-2′′, H-6′′); ^{13}C NMR (100 MHz, $CDCl_3$): δ 23.44 (C-7), 28.45 (C-6), 37.67 (C-3), 45.17 (C-4), 56.14 (-OCH_3), 71.04 (-OCH_2Ph), 89.56 (C-5), 110.54 (C-2′), 114.35 (C-5′), 119.06 (C-6′), 127.23 (C-2′′, C-6′′), 127.93 (C-4′′), 128.57 (C-3′′, C-5′′), 134.31 (C-1′), 136.85 (C-1′′), 147.69 (C-4′), 150.15 (C-3′), 174.88 (C-2); minor signals from *anti* conformer: ^1H NMR: δ 1.97 (d, *J* = 7.1 Hz, 3H, CH_3-7), 2.76 (dd, *J* = 18.1 and 9.5 Hz, one of CH_2-3), 3.07 (dd, *J* = 18.1 Hz and 9.5 Hz, 1H, one of CH_2-3), 3.46 (td, *J* = 9.5 and 7.1 Hz, 1H, H-4), 3.73 (dd, *J* = 7.1 and 2.4 Hz, 1H, H-5), 3.90 (s, 3H, -OCH_3), 5.30 (s, 2H, -OCH_2Ph), 6.85 (d, *J* = 8.1 Hz, 1H, H-5′); ^{13}C NMR: δ 25.42 (C-7), 29.02 (C-6), 37.04 (C-3), 47.41 (C-4), 89.27 (C-5), 110.70 (C-2′), 119.26 (C-6′), 132.07 (C-1′), 174.80 (C-2); IR (ATR): ν_{max} = 1786, 1517, 1454, 1254, 1142, 1030, 970, 848, 804, 746, 697, 644, 536 cm^{-1}; HRMS (ESI): *m*/*z* calcd for $C_{20}H_{21}IO_4$ $[M+Na]^+$: 475.0377; found: 475.0378.

3.8.3. 4-*r*-(4'-Benzyloxy-3'-methoxyphenyl)-5-*t*-iodo-6-*c*-methyltetrahydropyran-2-one **(7c)**

Yield 0.38 g (11%); white solid; mp 109-112 °C; R_f = 0.15 (hexane/ethyl acetate 4:1, *v*/*v*); ^1H NMR (400 MHz, $CDCl_3$): δ 1.74 (d, *J* = 6.2 Hz, 3H, CH_3-7), 2.65 (dd, *J* = 17.6 and 10.6 Hz, 1H, one of CH_2-3), 2.98 (dd, *J* = 17.6 and 6.6 Hz, 1H, one of CH_2-3), 3.43 (td, *J* = 10.6 and 6.6 Hz, 1H, H-4), 3.90 (s, 3H, -OCH_3), 4.00 (t, *J* = 10.6 Hz, H-5), 4.75 (dq, *J* = 10.6 and 6.2 Hz, 1H, H-6), 5.15 (s, 2H, -OCH_2Ph), 6.65 (dd, *J* = 8.0 and 2.2 Hz, 1H, H-6′), 6.67 (d, *J* = 2.2 Hz, 1H, H-2′), 6.87 (d, *J* = 8.0 Hz, 1H, H-5′), 7.31 (m, 1H, H-4′′), 7.35-7.40 (m, 2H, H-3′′, H-5′′), 7.42-7.46 (m, 2H, H-2′′, H-6′′); ^{13}C NMR (100 MHz, $CDCl_3$): δ 22.30 (C-7), 34.90 (C-5), 37.72 (C-3), 48.22 (C-4), 56.10 (-OCH_3), 70.99 (-OCH_2Ph), 81.00 (C-6), 110.46 (C-2′), 113.99 (C-5′), 118.90 (C-6′), 127.27 (C-2′′, C-6′′), 127.90 (C-4′′), 128.56 (C-3′′, C-5′′), 135.42 (C-1′), 136.90 (C-1′′), 147.79 (C-4′), 149.84 (C-3′), 169.73 (C-2); IR (ATR): ν_{max} = 1714, 1518, 1377, 1261, 1141, 1029, 971, 851, 810, 740, 699, 574 cm^{-1}; HRMS (ESI): m/z calcd for $C_{20}H_{21}IO_4$ $[M+Na]^+$: 475.0377; found: 475.0383.

3.9. Preparation of Bromolactones ***8a,b***

A solution of acid **6** (2.51 g, 7.70 mmol) and *N*-bromosuccinimide (1.89 g, 10.62 mmol) in THF (80 mL), with a few drops of acetic acid, was stirred at room temperature for 24 h. The mixture was then diluted with diethyl ether (40 mL) and washed with saturated $NaHCO_3$ solution and brine. The organic layer was dried over anhydrous $MgSO_4$. After solvent evaporation under reduced pressure, the product mixture was purified by flash chromatography (gradient elution from hexane to hexane/ethyl acetate 5:1, *v*/*v*). Two bromolactones, **8a** and **8b**, were isolated and characterized by the following data:

3.9.1. *Cis*-4-(4'-benzyloxy-3'-methoxyphenyl)-5-(1-bromoethyl)dihydrofuran-2-one **(8a)**

 doi:10.20944/preprints202507.1965.v1

Yield 1.12 g (35%); white solid; mp 125-128 °C; R_f = 0.39 (hexane/chloroform/methanol 8:2:1, *v*/*v*); ^{1}H NMR (400 MHz, $CDCl_3$): δ 1.76 (d, *J* = 6.6 Hz, 3H, CH_3-7), 2.71 (d, *J* = 17.5 Hz, 1H, one of CH_2-3), 3.09 (dd, *J* = 17.5 and 8.4 Hz, 1H, one of CH_2-3), 3.45 (dq, *J* = 10.4 and 6.6 Hz, 1H, H-6), 3.81 (dd, *J* = 8.4 and 5.1 Hz, 1H, H-4), 3.87 (s, 3H, -OCH_3), 4.64 (dd, *J* = 10.4 and 5.1 Hz, 1H, H-5), 5.14 (s, 2H, -OCH_2Ph), 6.68 (dd, *J* = 8.3 and 2.1 Hz, 1H, H-6′), 6.79 (d, *J* = 2.1 Hz, 1H, H-2′), 6.84 (d, *J* = 8.3 Hz, 1H, H-5′), 7.31 (m, 1H, H-4′′), 7.34-7.40 (m, 2H, H-3′′, H-5′′), 7.41-7.47 (m, 2H, H-2′′, H-6′′); ^{13}C NMR (100 MHz, $CDCl_3$): δ 23.26 (C-7), 38.29 (C-3), 43.64 (C-4), 45.54 (C-6), 56.02 (-OCH_3), 70.97 (-OCH_2Ph), 86.71 (C-5), 112.58 (C-2′), 113.83 (C-5′), 120.10 (C-6′), 127.30 (C-2′′, C-6′′), 127.93 (C-4′′), 128.57 (C-3′′, C-5′′), 130.19 (C-1′), 136.87 (C-1′′), 147.82 (C-4′), 149.34 (C-3′), 176.42 (C-2); IR (ATR): ν_{max} = 178, 1518, 1254, 1146, 1015, 966, 780, 747, 699 cm^{-1}; HRMS (ESI): m/z calcd for $C_{20}H_{21}BrO_4$ $[M+Na]^+$: 427.0515; found: 427.0522.

3.9.2. 4-*r*-(4'-Benzyloxy-3'-methoxyphenyl)-5-*t*-bromo-6-*c*-methyltetrahydropyran-2-one **(8b)**

Yield 0.26 g (8%); white solid; mp 132-134 °C; R_f = 0.33 (hexane/chloroform/methanol 8:2:1, *v*/*v*); ^{1}H NMR (400 MHz, $CDCl_3$): δ 1.65 (d, *J* = 6.2 Hz, 3H, CH_3-7), 2.70 (dd, *J* = 17.6 and 9.4 Hz, 1H, one of CH_2-3), 3.05 (dd, *J* = 17.6 and 6.9 Hz, 1H, one of CH_2-3), 3.40 (td, *J* = 9.4 and 6.9 Hz, 1H, H-4), 3.90 (s, 3H, -OCH_3), 3.91 (t, *J* = 9.4 Hz, H-5), 4.63 (dq, *J* = 9.4 and 6.2 Hz, 1H, H-6), 5.14 (s, 2H, -OCH_2Ph), 6.68 (dd, *J* = 8.1 and 2.1 Hz, 1H, H-6′), 6.71 (d, *J* = 2.1 Hz, 1H, H-2′), 6.87 (d, *J* = 8.1 Hz, 1H, H-5′), 7.31 (m, 1H, H-4′′), 7.34-7.40 (m, 2H, H-3′′, H-5′′), 7.41-7.46 (m, 2H, H-2′′, H-6′′); ^{13}C NMR (100 MHz, $CDCl_3$): δ 20.62 (C-7), 37.64 (C-3), 46.78 (C-4), 54.51 (C-5), 56.10 (-OCH_3), 71.00 (-OCH_2Ph), 79.59 (C-6), 110.66 (C-2′), 114.05 (C-5′), 119.00 (C-6′), 127.25 (C-2′′, C-6′′), 127.90 (C-4′′), 128.57 (C-3′′, C-5′′), 133.91 (C-1′), 136.93 (C-1′′), 147.81 (C-4′), 149.88 (C-3′), 169.45 (C-2); IR (ATR): ν_{max} = 1721, 1517, 1375, 1225, 1141, 1001, 972, 804, 758, 704 cm^{-1}; HRMS (ESI): *m*/*z* calcd for $C_{20}H_{21}BrO_4$ $[M+Na]^+$: 427.0515; found: 427.0517.

3.10. Preparation of Chlorolactones ***9a,b***

A solution of acid **6** (2.51 g, 7.70 mmol) and *N*-chlorosuccinimide (2.32 g, 17.37 mmol) in THF (80 mL), with a few drops of acetic acid, was stirred at room temperature for 24 h. The work-up procedure and isolation described in Section 3.9 were applied to isolate chlorolactones **9a** and **9b**, which were characterized by the following physical and spectral data:

3.10.1. *Cis*-4-(4'-benzyloxy-3'-methoxyphenyl)-5-(1-chloroethyl)dihydrofuran-2-one **(9a)**

Yield 0.28 g (10%); white solid; mp 81-84 °C; R_f = 0.37 (hexane/chloroform/methanol 8:2:1, *v*/*v*); ^{1}H NMR (400 MHz, $CDCl_3$): δ 1.56 (d, *J* = 6.5 Hz, 3H, CH_3-7), 2.71 (d, *J* = 17.6 and 0.8 Hz, 1H, one of CH_2-3), 3.07 (dd, *J* = 17.6 and 8.4 Hz, 1H, one of CH_2-3), 3.43 (dq, *J* = 10.1 and 6.5 Hz, 1H, H-6), 3.80 (dd, *J* = 8.4 and 5.2 Hz, 1H, H-4), 3.87 (s, 3H, -OCH_3), 4.49 (dd, *J* = 10.1 and 5.2 Hz, 1H, H-5), 5.14 (s, 2H, -OCH_2Ph), 6.66 (dd, *J* = 8.3 and 2.2 Hz, 1H, H-6′), 6.76 (d, *J* = 2.2 Hz, 1H, H-2′), 6.84 (d, *J* = 8.3 Hz, 1H, H-5′), 7.31 (m, 1H, H-4′′), 7.35-7.40 (m, 2H, H-3′′, H-5′′), 7.42-7.46 (m, 2H, H-2′′, H-6′′); ^{13}C NMR (100 MHz, $CDCl_3$): δ 22.38 (C-7), 37.94 (C-3), 43.13 (C-4), 53.93 (C-6), 56.02 (-OCH_3), 70.97 (-OCH_2Ph), 86.58 (C-5), 112.42 (C-2′), 113.82 (C-5′), 120.03 (C-6′), 127.29 (C-2′′, C-6′′), 127.92 (C-4′′), 128.57 (C-3′′, C-5′′), 130.30 (C-1′), 136.87 (C-1′′), 147.81 (C-4′), 149.37 (C-3′), 176.34 (C-2); IR (ATR): ν_{max} = 1789, 1516, 1454, 1238, 1144, 1019, 973, 780, 745, 698, 680 cm^{-1}; HRMS (ESI): *m*/*z* calcd for $C_{20}H_{21}O_4Cl$ $[M+H]^+$: 361.1207; found: 361.1206.

3.10.2. 4-*r*-(4'-Benzyloxy-3'-methoxyphenyl)-5-*t*-chloro-6-*c*-methyltetrahydropyran-2-one (**9b**)

Yield 0.5 g (18%); white solid; mp 93-96 °C; R_f = 0.24 (hexane/chloroform/methanol 8:2:1, *v*/*v*); ^{1}H NMR (400 MHz, $CDCl_3$): δ 1.60 (d, *J* = 6.2 Hz, 3H, CH_3-7), 2.72 (dd, *J* = 17.7 and 9.5 Hz, 1H, one of CH_2-3), 3.06 (dd, *J* = 17.7 and 7.0 Hz, 1H, one of CH_2-3), 3.29 (td, *J* = 9.5 and 7.0 Hz, 1H, H-4), 3.83 (t, *J* = 10.0 Hz, H-5), 3.90 (s, 3H, -OCH_3), 4.50 (dq, *J* = 10.0 and 6.2 Hz, 1H, H-6), 5.14 (s, 2H, -OCH_2Ph), 6.70 (dd,

 doi:10.20944/preprints202507.1965.v1

J = 8.1 and 2.2 Hz, 1H, H-6'), 6.72 (d, *J* = 2.2 Hz, 1H, H-2'), 6.87 (d, *J* = 8.1 Hz, 1H, H-5'), 7.31 (m, 1H, H-4''), 7.35-7.40 (m, 2H, H-3'', H-5''), 7.42-7.46 (m, 2H, H-2'', H-6''); ^{13}C NMR (100 MHz, $CDCl_3$): δ 19.66 (C-7), 37.21 (C-3), 46.31 (C-4), 56.09 (-OCH_3), 62.47 (C-5), 71.00 (-OCH_2Ph), 79.35 (C-6), 110.78 (C-2'), 114.08 (C-5'), 119.10 (C-6'), 127.24 (C-2'', C-6''), 127.90 (C-4''), 128.57 (C-3'', C-5''), 133.13 (C-1'), 136.93 (C-1''), 147.82 (C-4'), 149.89 (C-3'), 169.33 (C-2); IR (ATR): ν_{max} = 1732, 1511, 1258, 1219, 1139, 1016, 973, 796, 738, 696, 642 cm^{-1}; HRMS (ESI): *m*/*z* calcd for $C_{20}H_{21}O_4Cl$ [M+H]$^+$: 361.1207; found: 361.1205.

3.11. General Procedure for Benzyl Deprotection of Halolactones ***7a-c, 8a,b*** *and* ***9a,b***

Lactone **7-9** (1 equiv) was placed in a two-necked flask equipped with a nitrogen-filled balloon and dissolved in 10 mL of anhydrous methylene chloride. The flask was placed on a magnetic stirrer, and after complete dissolution of the substrate, anhydrous $FeCl_3$ (3 equiv) was added. The mixture was stirred at room temperature. After complete reaction of the substrate (30 min), the crude reaction mixture was filtered under reduced pressure through a Schott funnel, transferred to a separatory funnel, and washed with 1% orthophosphoric acid solution (3 × 10 mL). After phase separation, the aqueous layer was further washed with methylene chloride (3 × 15 mL). All combined organic layers were neutralized with saturated NaCl solution and dried over anhydrous $MgSO_4$. After filtration, the solvent was evaporated under reduced pressure using a rotary evaporator. The concentrated crude product was purified by flash chromatography. Gradient elution from hexane to hexane/ethyl acetate 9:2 (*v*/*v*) was used for lactones **10a**, **10b**, **12a**, and **12b**, while for lactone **11a** a gradient from hexane to hexane/ethyl acetate 3:1 (*v*/*v*) was applied. Reaction yields and the physical and spectral data of the deprotected halolactones are as follows:

3.11.1. *Cis*-4-(4'-hydroxy-3'-methoxyphenyl)-5-(1-iodoethyl)dihydrofuran-2-one **(10a)**

Obtained from lactone **7a** (1.81 g, 4 mmol) in yield 0.41 g (28%); white solid; mp 56-59 °C; R_f = 0.24 (hexane/ethyl acetate 3:1, *v*/*v*), ^{1}H NMR (400 MHz, $CDCl_3$): δ 2.01 (d, *J* = 6.8 Hz, 3H, CH_3-7), 2.70 (d, *J* = 17.5 Hz, 1H, one of CH_2-3), 3.11 (dd, *J* = 17.5 and 8.4 Hz, 1H, one of CH_2-3), 3.48 (dq, *J* = 10.9 and 6.8 Hz, 1H, H-6), 3.83 (dd, *J* = 8.4 and 5.0 Hz, 1H, H-4), 3.89 (s, 3H, -OCH_3), 4.78 (dd, *J* = 10.9 and 5.0 Hz, 1H, H-5), 5.62 (s, 1H, -OH), 6.74 (dd, *J* = 8.1 and 2.0 Hz, 1H, H-6'), 6.78 (d, *J* = 2.0 Hz, 1H, H-2'), 6.86 (d, *J* = 8.1 Hz, 1H, H-5'); ^{13}C NMR (100 MHz, $CDCl_3$): δ 23.72 (C-6), 25.53 (C-7), 38.91 (C-3), 44.66 (C-4), 56.01 (-OCH_3), 87.93 (C-5), 111.45 (C-2'), 114.64 (C-5'), 121.20 (C-6'), 128.94 (C-1'), 145.33 (C-4'), 146.34 (C-3'), 176.67 (C-2); IR (ATR): ν_{max} = 3367, 1762, 1518, 1178, 1129, 1033, 966, 846, 597, 527 cm^{-1}; HRMS (ESI): *m*/*z* calcd for $C_{13}H_{15}O_4I$ [M+H]$^+$: 363.0093; found: 363.0094.

3.11.2. *Trans*-4-(4'-hydroxy-3'-methoxyphenyl)-5-(1-iodoethyl)dihydrofuran-2-one **(10b)**

Obtained from lactone **7b** (0.87 g, 2.40 mmol) in yield 0.11 g (16%) and from lactone **7c** (0.38 g, 1.05 mmol) in yield 0.05 g (18%); white solid; mp 39-41 °C; R_f = 0.16 (hexane/ethyl acetate 3:1, *v*/*v*); ^{1}H NMR (600 MHz, $CDCl_3$): δ 1.87 (d, *J* = 7.1 Hz, 3H, CH_3-7), 2.64 (dd, *J* = 18.4 and 6.6 Hz, one of CH_2-3), 3.13 (dd, *J* = 18.4 and 10.1 Hz, 1H, one of CH_2-3), 3.56 (ddd, *J* = 10.1, 6.6 and 5.3 Hz, 1H, H-4), 3.90 (s, 3H, -OCH_3), 4.23 (t, *J* = 5.3 Hz, 1H, H-5), 4.37 (qd, *J* = 7.1 and 5.3 Hz, 1H, H-6), 5.61 (s, 1H, -OH), 6.71 (d, *J* = 2.1 Hz, 1H, H-2'), 6.76 (dd, *J* = 8.1 and 2.1 Hz, 1H, H-6'), 6.89 (d, *J* = 8.1 Hz, 1H, H-5'); ^{13}C NMR (150 MHz, $CDCl_3$): δ 23.48 (C-7), 28.38 (C-6), 37.81 (C-3), 45.26 (C-4), 56.05 (-OCH_3), 89.70 (C-5), 109.25 (C-2'), 115.00 (C-5'), 119.91 (C-6'), 133.26 (C-1'), 145.24 (C-4'), 147.07 (C-3'), 174.89 (C-2); IR (ATR): ν_{max} = 3406, 1770, 1516, 1269, 1148, 1026, 969, 816, 757, 596 cm^{-1}; HRMS (ESI): *m*/*z* calcd for $C_{13}H_{15}O_4I$ [M+H]$^+$: 363.0093; found: 363.0094.

3.11.3. *Cis*-5-(1-bromoethyl)-4-(4'-hydroxy-3'-methoxyphenyl)dihydrofuran-2-one **(11a)**

 doi:10.20944/preprints202507.1965.v1

Obtained from lactone **8a** (1.12 g, 3.55 mmol) in yield 0.24 g (28%); white solid; mp 43-46 °C; R_f = 0.27 (hexane/chloroform/methanol 8:2:1, *v*/*v*); Rt = 6.84 min; ^{1}H NMR (600 MHz, $CDCl_3$): δ 1.76 (d, *J* = 6.6 Hz, 3H, CH_3-7), 2.71 (d, *J* = 17.3 Hz, 1H, one of CH_2-3), 3.10 (dd, *J* = 17.3 and 8.5 Hz, 1H, one of CH_2-3), 3.46 (dq, *J* = 10.4 and 6.6 Hz, 1H, H-6), 3.81 (dd, *J* = 8.5 and 5.1 Hz, 1H, H-4), 3.88 (s, 3H, -OCH_3), 4.64 (dd, *J* = 10.4 and 5.1 Hz, 1H, H-5), 5.62 (s, 1H, -OH), 6.71 (dd, *J* = 8.1 and 2.1 Hz, 1H, H-6′), 6.73 (d, *J* = 2.1 Hz, 1H, H-2′), 6.87 (d, *J* = 8.1 Hz, 1H, H-5′); ^{13}C NMR (150 MHz, $CDCl_3$): δ 23.26 (C-7), 38.36 (C-3), 43.74 (C-4), 45.56 (C-6), 55.97 (-OCH_3), 86.76 (C-5), 111.23 (C-2′), 114.59 (C-5′), 121.00 (C-6′), 129.08 (C-1′), 145.32 (C-4′), 146.34 (C-3′), 176.47 (C-2); IR (ATR): ν_{max} = 3333, 1737, 1519, 1132, 967, 777, 703, 624 cm^{-1}; HRMS (ESI): *m*/*z* calcd for $C_{13}H_{15}O_4Br$ [M+H]$^+$: 315,0232; found: 315.0230.

3.11.4. *Cis*-5-(1-chloroethyl)-4-(4'-hydroxy-3'-methoxyphenyl)dihydrofuran-2-one **(12a)**

Obtained from lactone **9a** (0.28 g, 0.78 mmol) in yield 0.06 g (28%); white solid; mp 86-89 °C; R_f = 0.13 (hexane/chloroform/methanol 8:2:1, *v*/*v*); ^{1}H NMR (600 MHz, $CDCl_3$): δ 1.57 (d, *J* = 6.5 Hz, 3H, CH_3-7), 2.72 (d, *J* = 17.6 Hz, 1H, one of CH_2-3), 3.08 (dd, *J* = 17.6 and 8.5 Hz, 1H, one of CH_2-3), 3.45 (dq, *J* = 10.1 and 6.5 Hz, 1H, H-6), 3.80 (dd, *J* = 8.5 and 5.2 Hz, 1H, H-4), 3.88 (s, 3H, -OCH_3), 4.50 (dd, *J* = 10.1 and 5.2 Hz, 1H, H-5), 5.61 (s, 1H, -OH), 6.69-6.70 (two m, 2H, H-2′ and H-6′), 6.88 (d, *J* = 8.4 Hz, 1H, H-5′); ^{13}C NMR (150 MHz, $CDCl_3$): δ 22.38 (C-7), 38.02 (C-3), 43.30 (C-4), 53.96 (C-6), 55.97 (-OCH_3), 86.65 (C-5), 111.10 (C-6′), 114.60 (C-5′), 120.96 (C-2′), 129.21 (C-1′), 145.35 (C-4′), 146.41 (C-3′), 176.33 (C-2); IR (ATR): ν_{max} = 3422, 1763, 1517, 1266, 1188, 1128, 1018, 974, 838, 785, 632, 600 cm^{-1}; HRMS (ESI): *m*/*z* calcd for $C_{13}H_{15}O_4Cl$ [M-H]$^-$: 269.0581; found: 269.0573.

3.11.5. 5-*t*-Chloro-4-*r*-(4'-hydroxy-3'-methoxyphenyl)-6-*c*-methyltetrahydropyran-2-one **(12b)**

Obtained from lactone **9b** (0.50 g, 1.39 mmol) in yield 0.07 g (19%); white solid; mp 52-55 °C; R_f = 0.06 (hexane/chloroform/methanol 8:2:1, *v*/*v*); ^{1}H NMR (600 MHz, $CDCl_3$): δ 1.60 (d, *J* = 6.2 Hz, 3H, CH_3-7), 2.73 (dd, *J* = 17.8 and 10 Hz, 1H, one of CH_2-3), 3.06 (dd, *J* = 17.8 and 7.0 Hz, 1H, one of CH_2-3), 3.27 (td, *J* = 10.0 and 7.0 Hz, 1H, H-4), 3.83 (t, *J* = 10.0 Hz, H-5), 3.90 (s, 3H, -OCH_3), 4.50 (dq, *J* = 10.0 and 6.2 Hz, 1H, H-6), 5.62 (s, 1H, -OH), 6.68 (d, *J* = 2.0 Hz, 1H, H-2′), 6.72 (dd, *J* = 8.1 and 2.0 Hz, 1H, H-6′), 6.91 (d, *J* = 8.1 Hz, 1H, H-5′); ^{13}C NMR (150 MHz, $CDCl_3$): δ 19.76 (C-7), 37.33 (C-3), 46.44 (C-4), 55.97 (-OCH_3), 62.64 (C-5), 79.37 (C-6), 109.66 (C-2′), 115.04(C-5′), 119.84 (C-6′), 132.08 (C-1′), 145.30 (C-4′), 146.83 (C-3′), 169.30 (C-2); IR (ATR): ν_{max} = 3394, 1728, 1518, 1215, 1054, 1030, 975, 735, 643, 578 cm^{-1}; HRMS (ESI): *m*/*z* calcd for $C_{13}H_{15}O_4Cl$ [M+H]$^+$: 271.0737; found: 271.0740.

3.12. Antiproliferative Activity

3.12.1. Chemicals for Biological Tests

The RPMI-1640 (Roswell Park Memorial Institute), McCoy's 5A, Eagle's Minimum Essential Medium (EMEM), Dulbecco's Modified Eagle's Medium High Glucose (DMEM HG), L-glutamine (L-Glu), DMSO (biological grade), 3-(4,5-dimethylthiazol-2-yl)-2,5-diphenyltetrazolium bromide (MTT) were purchased from Sigma-Aldrich® (Steinheim, Germany). The Fetal Bovine Serum (FBS) and advanced RPMI medium were purchased from Gibco/ThermoFisher (Waltham, MA, USA). Antibiotics penicillin-streptomycin (PS) was purchased from Corning (NY, USA). The T-75 cell culture flasks (EasYFlask Nunclon Delta Surface) and 96-well plates were purchased from NUNC (Kamstrupvej, Denmark).

3.12.2. Cell Lines and Cell Cultures

The CLB70 cell line (canine chronic B-cell lymphocytic leukemia) was established at the Department of Pharmacology and Toxicology, Wrocław University of Environmental and Life Sciences [60]. The CLBL-1 cell line (canine B-cell lymphoma) was kindly provided by Dr. Barbara C. Rütgen from the Institute of Immunology, Department of Pathobiology, University of Veterinary

 doi:10.20944/preprints202507.1965.v1

Medicine, Vienna [61]. The T-24 (human bladder carcinoma), Caco-2 (human colorectal adenocarcinoma), and NIH/3T3 (mouse embryonic fibroblasts) cell lines were purchased from the American Type Culture Collection (ATCC, Rockville, MD, USA).

Cell cultures were maintained in their respective growth media, with fetal bovine serum (FBS) concentrations ranging from 10% to 20%, depending on the cell line. Penicillin-streptomycin (PS) and L-glutamine (L-Glu) were consistently added at 1% each to all media. CLB70 cells were cultured in RPMI ADVANCE medium supplemented with 20% FBS, while CLBL-1 cells were maintained in RPMI-1640 medium with 20% FBS. T-24 cells were cultured in McCoy's 5A medium with 10% FBS, and Caco-2 cells in Eagle's Minimum Essential Medium (EMEM) with 20% FBS. NIH/3T3 cells were maintained in high-glucose DMEM (DMEM HG) with 10% FBS. All cell cultures were grown in T-75 flasks under a humidified atmosphere at 37°C and 5% CO_2 and passaged every 3 days to maintain optimal cell density (70–80% confluence).

3.12.3. MTT Assay

Stock solutions used in the experiments were freshly prepared for each trial by dissolving the tested compounds in biological-grade DMSO. These stock solutions were then diluted with the culture medium appropriate for each specific cell line to achieve the desired final concentrations, which ranged from 3.125 to 100 μM. The final DMSO concentration in each well was maintained below 1%, a level generally considered non-toxic to cells [62]. The MTT assay was employed to evaluate the antiproliferative and cytotoxic effects of the compounds on cancer cell lines, following a previously described protocol with minor modifications [31]. Cells were seeded in 96-well plates at the following densities: 1.5×10^4 cells/mL (NIH/3T3), 2×10^4 cells/mL (T-24, Caco-2), and 3×10^5 cells/mL (CLB70, CLBL-1). Each plate included control wells with untreated cells and wells with vehicle controls (culture medium specific to each cell line).

After 72 h of treatment with the tested compounds, 10 μL of 3-(4,5-dimethylthiazol-2-yl)-2,5-diphenyltetrazolium bromide (MTT) solution (5 mg/mL) was added to each well. The cells were subsequently incubated with MTT for an additional 3 h to allow the formation of formazan crystals. Following this, 40 μL of lysis buffer (composed of 46 g sodium dodecyl sulfate, 150 mL dimethylformamide, and 183.2 mL Milli-Q water) was added to each well to dissolve the formazan. After a 24 h incubation at room temperature, the optical density (OD) of the resulting formazan product was measured using a spectrophotometric microplate reader (Spark, Tecan, Männedorf, Switzerland) at 570 nm. To correct for background absorbance and minimize potential measurement artifacts, a reference wavelength of 630 nm, at which formazan exhibits negligible absorbance, was used.

The results were determined from three independent experiments (four wells each) and presented as mean IC_{50} value±SD from at least four independent experiments, each performed in quadruplicate. IC_{50} values (the concentration of the compound required to inhibit 50% of cell growth) were calculated from dose-response curves.

3.13. Cytototoxicity Toward Red Blood Cells (RBCs)

To evaluate the hemolytic potential and cytotoxicity of the tested compounds, a quantitative hemolysis assay was conducted using human red blood cells (RBCs), following the method described by Pruchnik et al. (2018), with minor modifications [63].

RBCs were obtained from healthy donors through the Blood Donation Center in Wrocław. In accordance with Polish law, the use of erythrocytes from blood centers for experimental purposes does not require approval from an ethics committee. The collected RBCs were gently resuspended and washed three times with cold isotonic phosphate-buffered saline (PBS, pH 7.4) to remove plasma and cellular debris.

All tested compounds were dissolved in biological-grade DMSO. A series of working solutions was prepared by diluting the stock solutions to final concentrations of 6.25, 12.50, 25, 50, 100, and

 doi:10.20944/preprints202507.1965.v1

200 μM. The DMSO content in all experimental and control samples did not exceed 1% (v/v). Control samples contained no tested compounds, while vehicle control samples contained DMSO at the same concentration as the treated samples. Positive control samples (A_{100}%) were prepared by inducing complete hemolysis with Milli-Q water. All experiments were performed in triplicate, with three independent replicates for each condition.

The erythrocyte suspension was adjusted to a final hematocrit of 1.2% in all test tubes, with a total sample volume of 1 mL. Samples were incubated at 37 °C under static conditions for 2, 24, and h to assess both short- and long-term cytotoxic effects.

Following incubation, all samples were centrifuged at 5000 rpm for 3 minutes at room temperature. The supernatants were carefully transferred to a 96-well plate, and the absorbance of free hemoglobin was measured at 540 nm using a UV-Vis microplate spectrophotometer (EPOCH, BioTek, Santa Clara, CA, USA). The degree of *in vitro* hemolysis was calculated based on the amount of released hemoglobin relative to that in the completely hemolyzed positive control sample, according to the following formula:

$$H\,[\%] = \frac{A_S}{A_{100\%}} \times 100\%,$$

where H [%] is the percentage of erythrocyte hemolysis, A_s is absorbance of hemoglobin in supernatant at 540 nm, and $A_{100\%}$ refers to the absorbance of hemoglobin in the supernatant following complete hemolysis of the erythrocytes.

4. Conclusions

This study presents the design, synthesis, and biological evaluation of five novel vanillin-derived γ-halo-δ-lactones and δ-halo-γ-lactones bearing a phenolic substituent at the β-position, obtained via a seven-step synthetic pathway. The compounds demonstrated potent and selective antiproliferative activity against both canine (CLBL-1, CLB70) and human (T-24, Caco-2) cancer cell lines, while exhibiting no cytotoxic effects on normal mouse fibroblasts (NIH/3T3). Hemolysis assays further confirmed their safety profile, indicating no toxicity toward human red blood cells (RBCs) and preservation of erythrocyte membrane integrity. Among the tested compounds, *trans* δ-iodo-γ-lactone **10b** showed the most promising biological activity. In addition to their antiproliferative properties, all halolactone derivatives will be subjected to further studies to evaluate their potential antioxidant and anti-inflammatory activities, as their structural features suggest broader, multi-target biological relevance.

Future research will aim first to elucidate the molecular basis of the selective antiproliferative activity exhibited by compound **10b**, including a detailed investigation of its anticancer mechanism of action. Understanding these fundamental aspects will be critical to rationally guide further optimization and application. Subsequently, efforts will focus on the design and synthesis of phospholipid-based liposomal nanocarriers incorporating compound **10b** to enhance its targeted delivery and therapeutic efficacy against cancer cells.

Supplementary Materials: The following supporting information can be downloaded at the website of this paper posted on Preprints.org. Figure S1: ^{1}H NMR spectrum of benzylvanillin **(2)**; Figure S2: ^{13}C NMR spectrum of benzylvanillin **(2)**; Figure S3: DEPT 135 NMR spectrum of benzylvanillin **(2)**; Figure S4: COSY spectrum of benzylvanillin **(2)**; Figure S5: HMQC spectrum of benzylvanillin **(2)**; Figure S6: HMBC spectrum of benzylvanillin **(2)**; Figure S7: ^{1}H NMR spectrum of (*E*)-4-(4'-(benzyloxy-3'-methoxyphenyl)but-3-en-2-one **(3)**; Figure S8: ^{13}C NMR spectrum of (*E*)-4-(4'-(benzyloxy-3'-methoxyphenyl)but-3-en-2-one **(3)**; Figure S9: DEPT 135 NMR spectrum of (*E*)-4-(4'-(benzyloxy-3'-methoxyphenyl)but-3-en-2-one **(3)**; Figure S10: COSY spectrum of (*E*)-4-(4'-(benzyloxy-3'-methoxyphenyl)but-3-en-2-one **(3)**; Figure S11: HMQC spectrum of (*E*)-4-(4'-(benzyloxy-3'-methoxyphenyl)but-3-en-2-one **(3)**; Figure S12: HMBC spectrum of (*E*)-4-(4'-(benzyloxy-3'-methoxyphenyl)but-

 doi:10.20944/preprints202507.1965.v1

3-en-2-one **(3)**; Figure S13: ^{1}H NMR spectrum of (*E*)-4-(4'-benzyloxy-3'-methoxyphenyl)but-3-en-2-ol **(4)**; Figure S14: ^{13}C NMR spectrum of (*E*)-4-(4'-benzyloxy-3'-methoxyphenyl)but-3-en-2-ol **(4)**; Figure S15: DEPT 135 NMR spectrum of (*E*)-4-(4'-benzyloxy-3'-methoxyphenyl)but-3-en-2-ol **(4)**; Figure S16: COSY spectrum of (*E*)-4-(4'-benzyloxy-3'-methoxyphenyl)but-3-en-2-ol **(4)**; Figure S17: HMQC spectrum of (*E*)-4-(4'-benzyloxy-3'-methoxyphenyl)but-3-en-2-ol **(4)**; Figure S18: HMBC spectrum of (*E*)-4-(4'-benzyloxy-3'-methoxyphenyl)but-3-en-2-ol **(4)**; Figure S19: ^{1}H NMR spectrum of (*E*)-3-(4'-benzyloxy-3'-methoxyphenyl)hex-4-enoate **(5)**; Figure S20: ^{13}C NMR spectrum of (*E*)-3-(4'-benzyloxy-3'-methoxyphenyl)hex-4-enoate **(5)**; Figure S21: DEPT 135 NMR spectrum of (*E*)-3-(4'-benzyloxy-3'-methoxyphenyl)hex-4-enoate **(5)**; Figure S22: COSY spectrum of (*E*)-3-(4'-benzyloxy-3'-methoxyphenyl)hex-4-enoate **(5)**; Figure S23: HMQC spectrum of (*E*)-3-(4'-benzyloxy-3'-methoxyphenyl)hex-4-enoate **(5)**; Figure S24: HMBC spectrum of (*E*)-3-(4'-benzyloxy-3'-methoxyphenyl)hex-4-enoate **(5)**; Figure S25: ^{1}H NMR spectrum of (*E*)-3-(4'-benzyloxy-3'-methoxyphenyl)hex-4-enoic acid **(6)**; Figure S26: ^{13}C NMR spectrum of (*E*)-3-(4'-benzyloxy-3'-methoxyphenyl)hex-4-enoic acid **(6)**; Figure S27: DEPT 135 NMR spectrum of (*E*)-3-(4'-benzyloxy-3'-methoxyphenyl)hex-4-enoic acid **(6)**; Figure S28: COSY spectrum of (*E*)-3-(4'-benzyloxy-3'-methoxyphenyl)hex-4-enoic acid **(6)**; Figure S29: HMQC spectrum of (*E*)-3-(4'-benzyloxy-3'-methoxyphenyl)hex-4-enoic acid **(6)**; Figure S30: HMBC spectrum of (*E*)-3-(4'-benzyloxy-3'-methoxyphenyl)hex-4-enoic acid **(6)**; Figure S31: ^{1}H NMR spectrum of *cis*-4-(4'-benzyloxy-3'-methoxyphenyl)-5-(1-iodoethyl)dihydrofuran-2-one **(7a)**; Figure S32: ^{13}C NMR spectrum of *cis*-4-(4'-benzyloxy-3'-methoxyphenyl)-5-(1-iodoethyl)dihydrofuran-2-one **(7a)**; Figure S33: DEPT NMR spectrum of *cis*-4-(4'-benzyloxy-3'-methoxyphenyl)-5-(1-iodoethyl)dihydrofuran-2-one **(7a)**; Figure S34: COSY spectrum of *cis*-4-(4'-benzyloxy-3'-methoxyphenyl)-5-(1-iodoethyl)dihydrofuran-2-one **(7a)**; Figure S35: HMQC spectrum of *cis*-4-(4'-benzyloxy-3'-methoxyphenyl)-5-(1-iodoethyl)dihydrofuran-2-one **(7a)**; Figure S36: HMBC spectrum of *cis*-4-(4'-benzyloxy-3'-methoxyphenyl)-5-(1-iodoethyl)dihydrofuran-2-one **(7a)**; Figure S37: ^{1}H NMR spectrum of *trans*-4-(4'-benzyloxy-3'-methoxyphenyl)-5-(1-iodoethyl)dihydrofuran-2-one **(7b)**; Figure S38: ^{13}C NMR spectrum of *trans*-4-(4'-benzyloxy-3'-methoxyphenyl)-5-(1-iodoethyl)dihydrofuran-2-one **(7b)**; Figure S39: DEPT 135 NMR spectrum of *trans*-4-(4'-benzyloxy-3'-methoxyphenyl)-5-(1-iodoethyl)dihydrofuran-2-one **(7b)**; Figure S40: COSY spectrum of *trans*-4-(4'-benzyloxy-3'-methoxyphenyl)-5-(1-iodoethyl)dihydrofuran-2-one **(7b)**; Figure S41: HMQC spectrum of *trans*-4-(4'-benzyloxy-3'-methoxyphenyl)-5-(1-iodoethyl)dihydrofuran-2-one **(7b)**; Figure S42: HMBC spectrum of *trans*-4-(4'-benzyloxy-3'-methoxyphenyl)-5-(1-iodoethyl)dihydrofuran-2-one **(7b)**; Figure S43: ^{1}H NMR spectrum of 4-*r*-(4'-benzyloxy-3'-methoxyphenyl)-5-*t*-iodo-6-*c*-methyltetrahydropyran-2-one **(7c)**; Figure S44: ^{13}C NMR spectrum of 4-*r*-(4'-benzyloxy-3'-methoxyphenyl)-5-*t*-iodo-6-*c*-methyltetrahydropyran-2-one **(7c)**; Figure S45: DEPT 135 NMR spectrum of 4-*r*-(4'-benzyloxy-3'-methoxyphenyl)-5-*t*-iodo-6-*c*-methyltetrahydropyran-2-one **(7c)**; Figure S46: COSY spectrum of 4-*r*-(4'-benzyloxy-3'-methoxyphenyl)-5-*t*-iodo-6-*c*-methyltetrahydropyran-2-one **(7c)**; Figure S47: HMQC spectrum of 4-*r*-(4'-benzyloxy-3'-methoxyphenyl)-5-*t*-iodo-6-*c*-methyltetrahydropyran-2-one **(7c)**; Figure S48: HMBC spectrum of 4-*r*-(4'-benzyloxy-3'-methoxyphenyl)-5-*t*-iodo-6-*c*-methyltetrahydropyran-2-one **(7c)**; Figure S49: ^{1}H NMR spectrum of *cis*-4-(4'-benzyloxy-3'-methoxyphenyl)-5-(1-bromoethyl)dihydrofuran-2-one **(8a)**; Figure S50: ^{13}C NMR spectrum of *cis*-4-(4'-benzyloxy-3'-methoxyphenyl)-5-(1-bromoethyl)dihydrofuran-2-one **(8a)**; Figure S51: DEPT 135 NMR spectrum of *cis*-4-(4'-benzyloxy-3'-methoxyphenyl)-5-(1-bromoethyl)dihydrofuran-2-one **(8a)**; Figure S52: COSY spectrum of *cis*-4-(4'-benzyloxy-3'-methoxyphenyl)-5-(1-bromoethyl)dihydrofuran-2-one **(8a)**; Figure S53: HMQC spectrum of *cis*-4-(4'-benzyloxy-3'-methoxyphenyl)-5-(1-bromoethyl)dihydrofuran-2-one **(8a)**; Figure S54: HMBC spectrum of *cis*-4-(4'-benzyloxy-3'-methoxyphenyl)-5-(1-bromoethyl)dihydrofuran-2-one **(8a)**; Figure S55: ^{1}H NMR spectrum of 4-*r*-(4'-benzyloxy-3'-methoxyphenyl)-5-*t*-bromo-6-*c*-methyltetrahydropyran-2-one **(8b)**; Figure S56: ^{13}C NMR spectrum of 4-*r*-(4'-benzyloxy-3'-methoxyphenyl)-5-*t*-bromo-6-*c*-methyltetrahydropyran-2-one **(8b)**; Figure S57: DEPT 135 NMR spectrum of 4-*r*-(4'-benzyloxy-3'-

 doi:10.20944/preprints202507.1965.v1

methoxyphenyl)-5-*t*-bromo-6-*c*-methyltetrahydropyran-2-one **(8b)**; Figure S58: COSY spectrum of 4-*r*-(4'-benzyloxy-3'-methoxyphenyl)-5-*t*-bromo-6-*c*-methyltetrahydropyran-2-one **(8b)**; Figure S59: HMQC spectrum of 4-*r*-(4'-benzyloxy-3'-methoxyphenyl)-5-*t*-bromo-6-*c*-methyltetrahydropyran-2-one **(8b)**; Figure S60: HMBC spectrum of 4-*r*-(4'-benzyloxy-3'-methoxyphenyl)-5-*t*-bromo-6-*c*-methyltetrahydropyran-2-one **(8b)**; Figure S61: ^{1}H NMR spectrum of *cis*-4-(4'-benzyloxy-3'-methoxyphenyl)-5-(1-chloroethyl)dihydrofuran-2-one **(9a)**; Figure S62: ^{13}C NMR spectrum of *cis*-4-(4'-benzyloxy-3'-methoxyphenyl)-5-(1-chloroethyl)dihydrofuran-2-one **(9a)**; Figure S63: DEPT 135 NMR spectrum of *cis*-4-(4'-benzyloxy-3'-methoxyphenyl)-5-(1-chloroethyl)dihydrofuran-2-one **(9a)**; Figure S64: COSY spectrum of *cis*-4-(4'-benzyloxy-3'-methoxyphenyl)-5-(1-chloroethyl)dihydrofuran-2-one **(9a)**; Figure S65: HMQC spectrum of *cis*-4-(4'-benzyloxy-3'-methoxyphenyl)-5-(1-chloroethyl)dihydrofuran-2-one **(9a)**; Figure S66: HMBC spectrum of *cis*-4-(4'-benzyloxy-3'-methoxyphenyl)-5-(1-chloroethyl)dihydrofuran-2-one **(9a)**; Figure S67: ^{1}H NMR spectrum of 4-*r*-(4'-benzyloxy-3'-methoxyphenyl)-5-*t*-chloro-6-*c*-methyltetrahydropyran-2-one **(9b)**; Figure S68: ^{13}CNMR spectrum of 4-*r*-(4'-benzyloxy-3'-methoxyphenyl)-5-*t*-chloro-6-*c*-methyltetrahydropyran-2-one **(9b)**; Figure S69: DEPT 135 NMR spectrum of 4-*r*-(4'-benzyloxy-3'-methoxyphenyl)-5-*t*-chloro-6-*c*-methyltetrahydropyran-2-one **(9b)**; Figure S70: COSY spectrum of 4-*r*-(4'-benzyloxy-3'-methoxyphenyl)-5-*t*-chloro-6-*c*-methyltetrahydropyran-2-one **(9b)**; Figure S71: HMQC spectrum of 4-*r*-(4'-benzyloxy-3'-methoxyphenyl)-5-*t*-chloro-6-*c*-methyltetrahydropyran-2-one **(9b)**; Figure S72: HMBC spectrum of 4-*r*-(4'-benzyloxy-3'-methoxyphenyl)-5-*t*-chloro-6-*c*-methyltetrahydropyran-2-one **(9b)**; Figure S73: ^{1}H NMR spectrum of *cis*-4-(4'-hydroxy-3'-methoxyphenyl)-5-(1-iodoethyl)dihydrofuran-2-one **(10a)**; Figure S74: ^{13}C NMR spectrum of *cis*-4-(4'-hydroxy-3'-methoxyphenyl)-5-(1-iodoethyl)dihydrofuran-2-one **(10a)**; Figure S75: DEPT 135 NMR spectrum of *cis*-4-(4'-hydroxy-3'-methoxyphenyl)-5-(1-iodoethyl)dihydrofuran-2-one **(10a)**; Figure S76: COSY spectrum of *cis*-4-(4'-hydroxy-3'-methoxyphenyl)-5-(1-iodoethyl)dihydrofuran-2-one **(10a)**; Figure S77: HMQC spectrum of *cis*-4-(4'-hydroxy-3'-methoxyphenyl)-5-(1-iodoethyl)dihydrofuran-2-one **(10a)**; Figure S78: HMBC spectrum of *cis*-4-(4'-hydroxy-3'-methoxyphenyl)-5-(1-iodoethyl)dihydrofuran-2-one **(10a)**; Figure S79: ^{1}H NMR spectrum of *trans*-4-(4'-hydroxy-3'-methoxyphenyl)-5-(1-iodoethyl)dihydrofuran-2-one **(10b)**; Figure S80: ^{13}C NMR spectrum of *trans*-4-(4'-hydroxy-3'-methoxyphenyl)-5-(1-iodoethyl)dihydrofuran-2-one **(10b)**; Figure S81: DEPT 135 NMR spectrum of *trans*-4-(4'-hydroxy-3'-methoxyphenyl)-5-(1-iodoethyl)dihydrofuran-2-one **(10b)**; Figure S82: COSY spectrum of *trans*-4-(4'-hydroxy-3'-methoxyphenyl)-5-(1-iodoethyl)dihydrofuran-2-one **(10b)**; Figure S83: HMQC spectrum of *trans*-4-(4'-hydroxy-3'-methoxyphenyl)-5-(1-iodoethyl)dihydrofuran-2-one **(10b)**; Figure S84: HMBC spectrum of *trans*-4-(4'-hydroxy-3'-methoxyphenyl)-5-(1-iodoethyl)dihydrofuran-2-one **(10b)**; Figure S85: ^{1}H NMR spectrum of *cis*-5-(1-bromoethyl)-4-(4'-hydroxy-3'-methoxyphenyl)dihydrofuran-2-one **(11a)**; Figure S86: ^{13}C NMR spectrum of *cis*-5-(1-bromoethyl)-4-(4'-hydroxy-3'-methoxyphenyl)dihydrofuran-2-one **(11a)**; Figure S87: DEPT 135 NMR spectrum of *cis*-5-(1-bromoethyl)-4-(4'-hydroxy-3'-methoxyphenyl)dihydrofuran-2-one **(11a)**; Figure S88: COSY spectrum of *cis*-5-(1-bromoethyl)-4-(4'-hydroxy-3'-methoxyphenyl)dihydrofuran-2-one **(11a)**; Figure S89: HMQC spectrum of *cis*-5-(1-bromoethyl)-4-(4'-hydroxy-3'-methoxyphenyl)dihydrofuran-2-one **(11a)**; Figure S90: HMBC spectrum of *cis*-5-(1-bromoethyl)-4-(4'-hydroxy-3'-methoxyphenyl)dihydrofuran-2-one **(11a)**; Figure S91: ^{1}H NMR spectrum of *cis*-5-(1-chloroethyl)-4-(4'-hydroxy-3'-methoxyphenyl)dihydrofuran-2-one **(12a)**; Figure S92: ^{13}C NMR spectrum of *cis*-5-(1-chloroethyl)-4-(4'-hydroxy-3'-methoxyphenyl)dihydrofuran-2-one **(12a)**;
Figure S93: DEPT 135 NMR spectrum of *cis*-5-(1-chloroethyl)-4-(4'-hydroxy-3'-methoxyphenyl)dihydrofuran-2-one **(12a)**; Figure S94: COSY spectrum of *cis*-5-(1-chloroethyl)-4-(4'-hydroxy-3'-methoxyphenyl)dihydrofuran-2-one **(12a)**; Figure S95: HMQC spectrum of *cis*-5-(1-chloroethyl)-4-(4'-hydroxy-3'-methoxyphenyl)dihydrofuran-2-one **(12a)**; Figure S96: HMBC spectrum of *cis*-5-(1-chloroethyl)-4-(4'-hydroxy-3'-methoxyphenyl)dihydrofuran-2-one **(12a)**; Figure S97: ^{1}H NMR spectrum of 5-*t*-chloro-4-*r*-(4'-hydroxy-3'-methoxyphenyl)-6-*c*-methyltetrahydropyran-2-one **(12b)**; Figure S98: ^{13}C NMR spectrum of 5-*t*-chloro-4-*r*-(4'-hydroxy-3'-

 doi:10.20944/preprints202507.1965.v1

methoxyphenyl)-6-*c*-methyltetrahydropyran-2-one **(12b)**; Figure S99: DEPT 135 NMR spectrum of 5-*t*-chloro-4-*r*-(4'-hydroxy-3'-methoxyphenyl)-6-*c*-methyltetrahydropyran-2-one **(12b)**; Figure S100: COSY spectrum of 5-*t*-chloro-4-*r*-(4'-hydroxy-3'-methoxyphenyl)-6-*c*-methyltetrahydropyran-2-one **(12b)**; Figure S101: HMQC spectrum of 5-*t*-chloro-4-*r*-(4'-hydroxy-3'-methoxyphenyl)-6-*c*-methyltetrahydropyran-2-one **(12b)**; Figure S102: HMBC spectrum of 5-*t*-chloro-4-*r*-(4'-hydroxy-3'-methoxyphenyl)-6-*c*-methyltetrahydropyran-2-one **(12b)**; Figure S103: IR spectrum of benzylvanillin **(2)**; Figure S104: IR spectrum of (*E*)-4-(4'-(benzyloxy-3'-methoxyphenyl)but-3-en-2-one **(3)**; Figure S105: IR spectrum of (*E*)-4-(4'-benzyloxy-3'-methoxyphenyl)but-3-en-2-ol **(4)**; Figure S106: IR spectrum of (*E*)-3-(4'-benzyloxy-3'-methoxyphenyl)hex-4-enoate **(5)**; Figure S107: IR spectrum of (*E*)-3-(4'-benzyloxy-3'-methoxyphenyl)hex-4-enoic acid **(6)**; Figure S108: IR spectrum of *cis*-4-(4'-benzyloxy-3'-methoxyphenyl)-5-(1-iodoethyl)dihydrofuran-2-one **(7a)**; Figure S109: IR spectrum of *trans*-4-(4'-benzyloxy-3'-methoxyphenyl)-5-(1-iodoethyl)dihydrofuran-2-one **(7b)**; Figure S110: IR spectrum of 4-*r*-(4'-benzyloxy-3'-methoxyphenyl)-5-*t*-iodo-6-*c*-methyltetrahydropyran-2-one **(7c)**; Figure S111: IR spectrum of *cis*-4-(4'-benzyloxy-3'-methoxyphenyl)-5-(1-bromoethyl)dihydrofuran-2-one **(8a)**; Figure S112: IR spectrum of 4-*r*-(4'-benzyloxy-3'-methoxyphenyl)-5-*t*-bromo-6-*c*-methyltetrahydropyran-2-one **(8b)**; Figure S113: IR spectrum of *cis*-4-(4'-benzyloxy-3'-methoxyphenyl)-5-(1-chloroethyl)dihydrofuran-2-one **(9a)**; Figure S114: IR spectrum of 4-*r*-(4'-benzyloxy-3'-methoxyphenyl)-5-*t*-chloro-6-*c*-methyltetrahydropyran-2-one **(9b)**; Figure S115: IR spectrum of *cis*-4-(4'-hydroxy-3'-methoxyphenyl)-5-(1-iodoethyl)dihydrofuran-2-one **(10a)**; Figure S116: IR spectrum of *trans*-4-(4'-hydroxy-3'-methoxyphenyl)-5-(1-iodoethyl)dihydrofuran-2-one **(10b)**; Figure S117: IR spectrum of *cis*-5-(1-bromoethyl)-4-(4'-hydroxy-3'-methoxyphenyl)dihydrofuran-2-one **(11a)**; Figure S118: IR spectrum of *cis*-5-(1-chloroethyl)-4-(4'-hydroxy-3'-methoxyphenyl)dihydrofuran-2-one **(12a)**; Figure S119: IR spectrum of 5-*t*-chloro-4-*r*-(4'-hydroxy-3'-methoxyphenyl)-6-*c*-methyltetrahydropyran-2-one **(12b)**;

Author Contributions: Conceptualization, A.D. W.G. and H.P.; methodology, W.G. H.P. and A.P.; writing-original draft, A.D.; writing-review and editing, W.G. H.P., A.W.; visualization, A.D. A.W. and J.S-Z., investigation: A.D. J.S-Z. A.W. E.D. and G.M.; supervision, W.G. and H.P. All authors have read and agreed to the published version of the manuscript.

Funding: This research was founded by the Wrocław University of Environmental and Life Sciences (Poland) as the Ph.D. research program number N020/0003/23 „Bon doktoranta SD UPWr", from the subsidy increased by the minister responsible for higher education and science for the period 2020-2026 in the amount of 2% of the subsidy referred to Art. 387 (3) of the Act of 20 July 2018 – Law on Higher Education and Science, obtained in 2019. The article is part of a PhD dissertation titled "Chemoenzymatic synthesis and determination of biological activity of lactones, vanillin derivatives and increasing the efficiency of their delivery to cancer cells", prepared during Doctoral School at the Wrocław University of Environmental and Life Sciences. The APC is financed by Wrocław University of Environmental and Life Sciences.

Institutional Review Board Statement: Not applicable.

Informed Consent Statement: Not applicable.

Data Availability Statement: The datasets used and/or analyzed during the current study are available from the corresponding author upon reasonable request.

Acknowledgments: During the preparation of this manuscript, the authors used ChatGPT (free version, OpenAI) for the purposes of language and grammar correction.

Conflicts of Interest: The authors declare no conflicts of interest.

 doi:10.20944/preprints202507.1965.v1

References

1. Sartori, S.K.; Diaz, M.A.N.; Diaz-Muñoz, G. Lactones: Classification, Synthesis, Biological Activities, and Industrial Applications. *Tetrahedron* **2021**, *84*, 132001, doi:10.1016/j.tet.2021.132001.
2. Fortuna, A.M.; de Riscala, E.C.; Catalan, C.A.N.; Gedris, T.E.; Herz, W. Sesquiterpene Lactones from Centaurea Tweediei. *Biochem Syst Ecol* **2001**, *29*, 967–971, doi:10.1016/s0305-1978(01)00042-4.
3. Sokovic, M.; Ciric, A.; Glamoclija, J.; Skaltsa, H. Biological Activities of Sesquiterpene Lactones Isolated from the Genus Centaurea L. (Asteraceae). *Curr Pharm Des* **2017**, *23*, 2767–2786, doi:10.2174/1381612823666170215113927.
4. Kumar, P.; Wallis, M.; Zhou, X.; Li, F.; Holland, D.C.; Reddell, P.; Münch, G.; Raju, R. Triplinones A-H: Anti-Inflammatory Arylalkenyl α,β-Unsaturated-δ-Lactones Isolated from the Leaves of Australian Rainforest Plant *Cryptocarya Triplinervis* (Lauraceae). *J Nat Prod* **2024**, *87*, 1817–1825, doi:10.1021/acs.jnatprod.4c00454.
5. Lohray, B.B.; Venkateswarlu, S. Intramolecular S_N2 Ring Opening of a Cyclic Sulfate: Synthesis of *Erythro*-(−)-6-Acetoxy-5-Hexadecanolide—a Major Component of Mosquito Oviposition Attractant Pheromone. *Tetrahedron: Asymmeto'* **1997**, *8*, 633–638, doi:10.1016/S0957-4166(97)00011-6.
6. McGlacken, G.P.; Fairlamb, I.J.S. 2-Pyrone Natural Products and Mimetics: Isolation, Characterisation and Biological Activity. *Nat Prod Rep* **2005**, *22*, 369–385, doi:10.1039/b416651p.
7. Zhang, L.; An, R.; Wang, J.; Sun, N.; Zhang, S.; Hu, J.; Kuai, J. Exploring Novel Bioactive Compounds from Marine Microbes. *Curr Opin Microbiol* **2005**, *8*, 276–281, doi:10.1016/j.mib.2005.04.008.
8. Karthikeyan, A.; Joseph, A.; Nair, B.G. Promising Bioactive Compounds from the Marine Environment and Their Potential Effects on Various Diseases. *Journal of Genetic Engineering and Biotechnology* **2022**, *20*, 1–38, doi:10.1186/s43141-021-00290-4.
9. Lee, K.-H.; Ibuka, T.; Wu, R.-Y.; Geissman, T.A. Structure–Antimicrobial Activity Relationships among the Sesquiterpene Lactones and Related Compounds. *Phytochemistry* **1977**, *16*, 1177–1181, doi:10.1016/S0031-9422(00)94355-3.
10. Kudumela, R.G.; Mazimba, O.; Masoko, P. Isolation and Characterisation of Sesquiterpene Lactones from *Schkuhria Pinnata* and Their Antibacterial and Anti-Inflammatory Activities. *South African Journal of Botany* **2019**, *126*, 340–344, doi:10.1016/j.sajb.2019.04.002.
11. Kowalczyk, P.; Gawdzik, B.; Trzepizur, D.; Szymczak, M.; Skiba, G.; Raj, S.; Kramkowski, K.; Lizut, R.; Ostaszewski, R. δ-Lactones—A New Class of Compounds That Are Toxic to *E. Coli* K12 and R2–R4 Strains. *Materials* **2021**, *14*, 2956, doi:10.3390/ma14112956.
12. Koszelewski, D.; Borys, F.; Brodzka, A.; Ostaszewski, R. Synthesis of Enantiomerically Pure 5,6-Dihydropyran-2-Ones via Chemoenzymatic Sequential DKR-RCM Reaction. *European J Org Chem* **2019**, *2019*, 1653–1658, doi:10.1002/ejoc.201801819.
13. Paço, A.; Brás, T.; Santos, J.O.; Sampaio, P.; Gomes, A.C.; Duarte, M.F. Anti-Inflammatory and Immunoregulatory Action of Sesquiterpene Lactones. *Molecules* **2022**, *27*, 1142, doi:10.3390/molecules27031142.
14. Dancewicz, K.; Szumny, A.; Wawrzeńczyk, C.; Gabryś, B. Repellent and Antifeedant Activities of Citral-Derived Lactones against the Peach Potato Aphid. *Int J Mol Sci* **2020**, *21*, 8029, doi:10.3390/ijms21218029.
15. Fraga, B.M.; Díaz, C.E.; Bailén, M.; González-Coloma, A. Sesquiterpene Lactones from *Artemisia Absinthium*. Biotransformation and Rearrangement of the Insect Antifeedant 3α-Hydroxypelenolide. *Plants* **2021**, *10*, 891, doi:10.3390/plants10050891.
16. Szczepanik, M.; Dams, I.; Wawrzeńczyk, C. Feeding Deterrent Activity of Terpenoid Lactones with the *p*-Menthane System Against the Colorado Potato Beetle (Coleoptera: Chrysomelidae). *Environ Entomol* **2005**, *34*, 1433–1440, doi:10.1603/0046-225X-34.6.1433.
17. Silva, L.C.; Tauhata, S.B.F.; Baeza, L.C.; Oliveira, C.M.A.; Kato, L.; Borges, C.L.; Soares, C.M.A.;; Pereira, M. Argentilactone Molecular Targets in *Paracoccidioides Brasiliensis* Identified by Chemoproteomics. *Antimicrob Agents Chemother* **2018**, *62*, e00737-18, doi:10.1128/AAC.00737-18.
18. Kaur, R.; Sharma, P.; Bhardwaj, U.; Kaur, R. Dehydrocostus Lactone: A Comprehensive Review on Its Isolation, Chemical Transformations, and Pharmacological Potential. *Discover Chemistry* **2025**, *2*, 131, doi:10.1007/s44371-025-00194-z.

 doi:10.20944/preprints202507.1965.v1

19. Zhi, X.Y.; Zhang, Y.; Li, Y.F.; Liu, Y.; Niu, W.P.; Li, Y.; Zhang, C.R.; Cao, H.; Hao, X.J.; Yang, C. Discovery of Natural Sesquiterpene Lactone 1-*O*-Acetylbritannilactone Analogues Bearing Oxadiazole, Triazole, or Imidazole Scaffolds for the Development of New Fungicidal Candidates. *J Agric Food Chem* **2023**, *71*, 11680–11691, doi:10.1021/acs.jafc.3c02497.
20. Rasul, A.; Parveen, S.; Ma, T. Costunolide: A Novel Anti-Cancer Sesquiterpene Lactone. *Bangladesh J Pharmacol* **2012**, *7*, 6–13, doi:10.3329/bjp.v7i1.10066.
21. Kim, D.Y.; Choi, B.Y. Costunolide—A Bioactive Sesquiterpene Lactone with Diverse Therapeutic Potential. *Int J Mol Sci* **2019**, *20*, 2926, doi:10.3390/ijms20122926.
22. Wzorek, A.; Kwiatkowska, M.; Hodorowicz, M.; Kalwat, K.; Arabski, M.; Płoszaj, P.; Gonciarz, W.; Omelaniuk, A.; Gmiter, D.; Kaca, W.; et al. Syntheses, Structures and Biological Activities of New Pyridinyl Lactones. *J Mol Struct* **2025**, *1319*, doi:10.1016/j.molstruc.2024.139534.
23. Kim, Y.; Sengupta, S.; Sim, T. Natural and Synthetic Lactones Possessing Antitumor Activities. *Int J Mol Sci* **2021**, *22*, 1052, doi:10.3390/ijms22031052.
24. Kamizela, A.; Gawdzik, B.; Urbaniak, M.; Lechowicz, Ł.; Białońska, A.; Kutniewska, S.E.; Gonciarz, W.; Chmiela, M. New γ-Halo-δ-Lactones and δ-Hydroxy-γ-Lactones with Strong Cytotoxic Activity. *Molecules* **2019**, *24*, 1875, doi:10.3390/molecules24101875.
25. Kamizela, A.; Gawdzik, B.; Urbaniak, M.; Lechowicz, Ł.; Białońska, A.; Gonciarz, W.; Chmiela, M. Synthesis, Characterization, Cytotoxicity, and Antibacterial Properties of *Trans*-γ-Halo-δ-Lactones. *ChemistryOpen* **2018**, *7*, 543–550, doi:10.1002/open.201800110.
26. Mereyala, H.B.; Joe, M. Cytotoxic Activity of Styryl Lactones and Their Derivatives. *Curr Med Chem Anticancer Agents* **2001**, *1*, 293–300, doi:10.2174/1568011013354606.
27. Albrecht, A.; Koszuk, J.F.; Modranka, J.; Różalski, M.; Krajewska, U.; Janecka, A.; Studzian, K.; Janecki, T. Synthesis and Cytotoxic Activity of γ-Aryl Substituted α-Alkylidene-γ-Lactones and α-Alkylidene-γ-Lactams. *Bioorg Med Chem* **2008**, *16*, 4872–4882, doi:10.1016/j.bmc.2008.03.035.
28. Park, S.; Kim, S.; Shin, D. Arylnaphthalene Lactones: Structures and Pharmacological Potentials. *Phytochemistry Reviews* **2021**, *20*, 1033–1054, doi:10.1007/s11101-020-09735-z.
29. Nguyen, T.K.; Thi Tran, L.T.; Truong Tan, T.; Pham, P.T.V.; Nguyen, L.T.K.; Nguyen, H.T.; Ho, D.V.; Tran, M.H. Isolation, Structural Elucidation, and Cytotoxic Activity Investigation of Novel Styryl-Lactone Derivatives from Goniothalamus Elegans: *In Vitro* and *in Silico* Studies. *RSC Adv* **2023**, *13*, 17587–17594, doi:10.1039/d3ra02646a.
30. Wzorek, A.; Gawdzik, B.; GŁadkowski, W.; Urbaniak, M.; Barańska, A.; Malińska, M.; Woźniak, K.; Kempinska, K.; Wietrzyk, J. Synthesis, Characterization and Antiproliferative Activity of β-Aryl-δ-Iodo-γ-Lactones. *J Mol Struct* **2013**, *1047*, 160–168, doi:10.1016/j.molstruc.2013.05.010.f
31. Gładkowski, W.; Skrobiszewski, A.; Mazur, M.; Siepka, M.; Pawlak, A.; Obmińska-Mrukowicz, B.; Białońska, A.; Poradowski, D.; Drynda, A.; Urbaniak, M. Synthesis and Anticancer Activity of Novel Halolactones with β-Aryl Substituents from Simple Aromatic Aldehydes. *Tetrahedron* **2013**, *69*, 10414–10423, doi:10.1016/j.tet.2013.09.094.
32. Gładkowski, W.; Skrobiszewski, A.; Mazur, M.; Gliszczyńska, A.; Czarnecka, M.; Pawlak, A.; Obmińska-Mrukowicz, B.; Maciejewska, G.; Białońska, A. Chiral δ-Iodo-γ-Lactones Derived from Cuminaldehyde, 2,5-Dimethylbenzaldehyde and Piperonal: Chemoenzymatic Synthesis and Antiproliferative Activity. *Tetrahedron Asymmetry* **2016**, *27*, 227–237, doi:10.1016/j.tetasy.2016.02.003.
33. Gładkowski, W.; Włoch, A.; Pawlak, A.; Sysak, A.; Białońska, A.; Mazur, M.; Mituła, P.; Maciejewska, G.; Obmińska-Mrukowicz, B.; Kleszczyńska, H. Preparation of Enantiomeric β-(2′,5′-Dimethylphenyl) Bromolactones, Their Antiproliferative Activity and Effect on Biological Membranes. *Molecules* **2018**, *23*, 3035, doi:10.3390/molecules23113035.
34. Pawlak, A.; Gładkowski, W.; Mazur, M.; Henklewska, M.; Obmińska-Mrukowicz, B.; Rapak, A. Optically Active Stereoisomers of 5-(1-Iodoethyl)-4-(4′-Isopropylphenyl)Dihydrofuran-2-One: The Effect of the Configuration of Stereocenters on Apoptosis Induction in Canine Cancer Cell Lines. *Chem Biol Interact* **2017**, *261*, 18–26, doi:10.1016/j.cbi.2016.11.013.
35. Pawlak, A.; Gładkowski, W.; Kutkowska, J.; Mazur, M.; Obmińska-Mrukowicz, B.; Rapak, A. Enantiomeric Trans β-Aryl-δ-Iodo-γ-Lactones Derived from 2,5-Dimethylbenzaldehyde Induce Apoptosis in Canine

 doi:10.20944/preprints202507.1965.v1

Lymphoma Cell Lines by Downregulation of Anti-Apoptotic Bcl-2 Family Members Bcl-xL and Bcl-2. *Bioorg Med Chem Lett* **2018**, *28*, 1171–1177, doi:10.1016/j.bmcl.2018.03.006.

36. Włoch, A.; Sengupta, P.; Szulc, N.; Kral, T.; Pawlak, A.; Henklewska, M.; Pruchnik, H.; Sykora, J.; Hof, M.; Gładkowski, W. Biophysical and Molecular Interactions of Enantiomeric Piperonal-Derived *Trans* β-Aryl-δ-Iodo-γ-Lactones with Cancer Cell Membranes, Protein and DNA: Implications for Anticancer Activity. *Int J Biol Macromol* **2025**, *303*, 140476, doi:10.1016/j.ijbiomac.2025.140476.
37. Włoch, A.; Stygar, D.; Bahri, F.; Bażanów, B.; Kuropka, P.; Chełmecka, E.; Pruchnik, H.; Gładkowski, W. Antiproliferative, Antimicrobial and Antiviral Activity of β-Aryl-δ-Iodo-γ-Lactones, Their Effect on Cellular Oxidative Stress Markers and Biological Membranes. *Biomolecules* **2020**, *10*, 1594, doi:10.3390/biom10121594.
38. Olatunde, A.; Mohammed, A.; Ibrahim, M.A.; Tajuddeen, N.; Shuaibu, M.N. Vanillin: A Food Additive with Multiple Biological Activities. *European Journal of Medicinal Chemistry Reports* **2022**, *5*, doi:10.1016/j.ejmcr.2022.100055.
39. Kafali, M.; Finos, M.A.; Tsoupras, A. Vanillin and Its Derivatives: A Critical Review of Their Anti-Inflammatory, Anti-Infective, Wound-Healing, Neuroprotective, and Anti-Cancer Health-Promoting Benefits. *Nutraceuticals* **2024**, *4*, 522–561, doi:10.3390/nutraceuticals4040030.
40. Arya, S.S.; Rookes, J.E.; Cahill, D.M.; Lenka, S.K. Vanillin: A Review on the Therapeutic Prospects of a Popular Flavouring Molecule. *Advances in Traditional Medicine* **2021**, *21*, 415–431, doi:10.1007/s13596-020-00531-w.
41. Yousuf, M.; Shamsi, A.; Queen, A.; Shahbaaz, M.; Khan, P.; Hussain, A.; Alajmi, M.F.; Rizwanul Haque, Q.M.; Imtaiyaz Hassan, M. Targeting Cyclin-Dependent Kinase 6 by Vanillin Inhibits Proliferation of Breast and Lung Cancer Cells: Combined Computational and Biochemical Studies. *J Cell Biochem* **2021**, *122*, 897–910, doi:10.1002/jcb.29921.
42. Liang, J.A.; Wu, S.L.; Lo, H.Y.; Hsiang, C.Y.; Ho, T.Y. Vanillin Inhibits Matrix Metalloproteinase-9 Expression through down-Regulation of Nuclear Factor-KB Signaling Pathway in Human Hepatocellular Carcinoma Cells. *Mol Pharmacol* **2009**, *75*, 151–157, doi:10.1124/mol.108.049502.
43. Ho, K.L.; Yazan, L.S.; Ismail, N.; Ismail, M. Apoptosis and Cell Cycle Arrest of Human Colorectal Cancer Cell Line HT-29 Induced by Vanillin. *Cancer Epidemiol* **2009**, *33*, 155–160, doi:10.1016/j.canep.2009.06.003.
44. Srinual, S.; Chanvorachote, P.; Pongrakhananon, V. Suppression of Cancer Stem-like Phenotypes in NCI-H460 Lung Cancer Cells by Vanillin through an Akt-Dependent Pathway. *Int J Oncol* **2017**, *50*, 1341–1351, doi:10.3892/ijo.2017.3879.
45. Park, E.J.; Lee, Y.M.; Oh, T.I.; Kim, B.M.; Lim, B.O.; Lim, J.H. Vanillin Suppresses Cell Motility by Inhibiting STAT3-Mediated HIF-1α MRNA Expression in Malignant Melanoma Cells. *Int J Mol Sci* **2017**, *18*, 532, doi:10.3390/ijms18030532.
46. 46. Gendron, D. Vanillin: A Promising Biosourced Building Block for the Preparation of Various Heterocycles. Front
    Chem **2022**, 10, 949355, doi:10.3389/fchem.2022.949355.
47. Yıldırım, M.; Ünver, H.; Necip, A.; Çimentepe, M. Design, Synthesis, and Biological Evaluation of Novel Vanillin-Derived Hydrazone Compounds with Antimicrobial, Anticancer, and Enzyme Inhibition Activities, along with Molecular Structure and Drug-Likeness Assessment. *Biochem Biophys Res Commun* **2025**, *775*, 152173, doi:10.1016/j.bbrc.2025.152173.
48. Scipioni, M.; Kay, G.; Megson, I.L.; Kong Thoo Lin, P. Synthesis of Novel Vanillin Derivatives: Novel Multi-Targeted Scaffold Ligands against Alzheimer's Disease. *Medchemcomm* **2019**, *10*, 764–777, doi:10.1039/c9md00048h.
49. Li, Z.H.; Liu, H.M.; Fan, Z.Y.; Pang, W.; Cheng, L.P. Design, Synthesis and Evaluation of Vanillin Derivatives as Dual-Target Inhibitors for the Treatment of Alzheimer's Disease. *Bioorg Med Chem* **2025**, *129*, 118296, doi:10.1016/j.bmc.2025.118296.
50. Carrasco-Gomez, R.; Keppner-Witter, S.; Hieke, M.; Lange, L.; Schneider, G.; Schubert-Zsilavecz, M.; Proschak, E.; Spänkuch, B. Vanillin-Derived Antiproliferative Compounds Influence Plk1 Activity. *Bioorg Med Chem Lett* **2014**, *24*, 5063–5069, doi:10.1016/j.bmcl.2014.09.015.

 doi:10.20944/preprints202507.1965.v1

51. Li, Y.; Manickam, G.; Ghoshal, A.; Subramaniam, P. More Efficient Palladium Catalyst for Hydrogenolysis of Benzyl Groups. *Synth Commun* **2006**, *36*, 925–928, doi:10.1080/00397910500466199.
52. Lanthier, C.; Payan, H.; Liparulo, I.; Hatat, B.; Lecoutey, C.; Since, M.; Davis, A.; Bergamini, C.; Claeysen, S.; Dallemagne, P.; et al. Novel Multi Target-Directed Ligands Targeting 5-HT_4 Receptors with in Cellulo Antioxidant Properties as Promising Leads in Alzheimer's Disease. *Eur J Med Chem* **2019**, *182*, 111596, doi:10.1016/j.ejmech.2019.111596.
53. 53. Gadhiya, S.; Madapa, S.; Kurtzman, T.; Alberts, I.L.; Ramsey, S.; Pillarsetty, N.K.; Kalidindi, T.; Harding, W.W. Tetrahydroprotoberberine Alkaloids with Dopamine and σ Receptor Affinity. Bioorg Med Chem 2016, 24, 2060–2071, doi:10.1016/j.bmc.2016.03.037.
54. Adinolfi, M.; Barone, G.; Guariniello, L.; Iadonisi, A. Facile Cleavage of Carbohydrate Benzyl Ethers and Benzylidene Acetals Using the $NaBrO_3/Na_2S_2O_4$ Reagent under Two-Phase Conditions. *Tetrahedron Lett* **1999**, *40*, 8439–8441.
55. Rodebaugh, R.; Debenham, J.S.; Fraser-Reid, B. Debenzylation of Complex Oligosaccharides Using Ferric Chloride. *Tetrahedron Lett* **1996**, *37*, 5477–5478, doi:10.1016/0040-4039(96)01169-0.
56. Giri, R.S.; Roy, S.; Dolai, G.; Manne, S.R.; Mandal, B. $FeCl_3$-Mediated Boc Deprotection: Mild Facile Boc-Chemistry in Solution and on Resin. *ChemistrySelect* **2020**, *5*, 2050–2056, doi:10.1002/slct.201904617.
57. Gładkowski, W.; Siepka, M.; Żarowska, B.; Białońska, A.; Gawdzik, B.; Urbaniak, M.; Wawrzeńczyk, C. Chalcone-Derived Lactones: Synthesis, Whole-Cell Biotransformation, and Evaluation of Their Antibacterial and Antifungal Activity. *Molecules* **2023**, *28*, 3800, doi:10.3390/molecules28093800.
58. Schrittwieser, J.H.; Resch, V.; Wallner, S.; Lienhart, W.D.; Sattler, J.H.; Resch, J.; MacHeroux, P.; Kroutil, W. Biocatalytic Organic Synthesis of Optically Pure (*S*)-Scoulerine and Berbine and Benzylisoquinoline Alkaloids. *Journal of Organic Chemistry* **2011**, *76*, 6703–6714, doi:10.1021/jo201056f.
59. Krishnamurty, H.G.; Ghosh S. Synthesis of Dihydrocurcumin. *Indian J Chem* **1986**, *25B*, 411–412.
60. Pawlak, A.; Ziolo, E.; Kutkowska, J.; Blazejczyk, A.; Wietrzyk, J.; Krupa, A.; Hildebrand, W.; Dziegiel, P.; Dzimira, S.; Obminska-Mrukowicz, B.; et al. A Novel Canine B-Cell Leukaemia Cell Line. Establishment, Characterisation and Sensitivity to Chemotherapeutics. *Vet Comp Oncol* **2017**, *15*, 1218–1231, doi:10.1111/vco.12257.
61. Rütgen, B.C.; Hammer, S.E.; Gerner, W.; Christian, M.; de Arespacochaga, A.G.; Willmann, M.; Kleiter, M.; Schwendenwein, I.; Saalmüller, A. Establishment and Characterization of a Novel Canine B-Cell Line Derived from a Spontaneously Occurring Diffuse Large Cell Lymphoma. *Leuk Res* **2010**, *34*, 932–938, doi:10.1016/j.leukres.2010.01.021.
62. Villarroel, A.; Duff, A.; Hu, T. DMSO Inhibits Human Cancer Cells and Downregulates the Expression of Cdk2 and Cyclin A. *The FASEB Journal* **2020**, *34*, 03158–1, doi:10.1096/fasebj.2020.34.s1.03158.
63. Pruchnik, H.; Włoch, A.; Bonarska-Kujawa, D.; Kleszczyńska, H. An In Vitro Study of the Effect of Cytotoxic Triorganotin Dimethylaminophenylazobenzoate Complexes on Red Blood Cells. *Journal of Membrane Biology* **2018**, *251*, 735–745, doi:10.1007/s00232-018-0051-x.